



Dietrich , K., Fiedler, I., Kurzyukova , A., López-Delgado , A. C., McGowan, L. M., Geurtzen , K., Hammond, C., Busse, B., & Knopf, F. (2021). Skeletal biology and disease modeling in zebrafish. *Journal of Bone and Mineral Research*, 36(3), 436-458.
<https://doi.org/10.1002/jbmr.4256>

Publisher's PDF, also known as Version of record

License (if available):
CC BY

Link to published version (if available):
[10.1002/jbmr.4256](https://doi.org/10.1002/jbmr.4256)

[Link to publication record in Explore Bristol Research](#)
PDF-document

This is the final published version of the article (version of record). It first appeared online via ASBMR at <https://doi.org/10.1002/jbmr.4256>. Please refer to any applicable terms of use of the publisher.

University of Bristol - Explore Bristol Research

General rights

This document is made available in accordance with publisher policies. Please cite only the published version using the reference above. Full terms of use are available:
<http://www.bristol.ac.uk/red/research-policy/pure/user-guides/ebr-terms/>

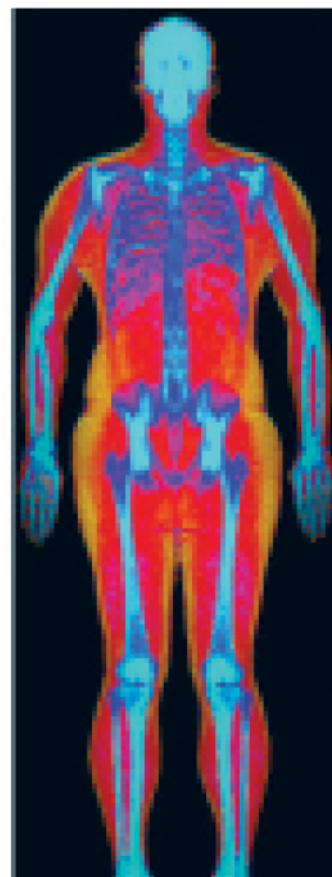
Powerful images. Clear answers.



Manage Patient's concerns about
Atypical Femur Fracture*



Vertebral Fracture Assessment –
a critical part of a complete
fracture risk assessment



Advanced Body Composition®
Assessment – the power to
see what's inside

Contact your Hologic rep today at BSHSalesSupportUS@hologic.com

PAID ADVERTISEMENT

*Incomplete Atypical Femur Fractures imaged with a Hologic densitometer, courtesy of Prof. Cheung, University of Toronto

ADS-02018 Rev 003 (10/19) Hologic Inc. ©2019 All rights reserved. Hologic, Advanced Body Composition, The Science of Sure and associated logos are trademarks and/or registered trademarks of Hologic, Inc., and/or its subsidiaries in the United States and/or other countries. This information is intended for medical professionals in the U.S. and other markets and is not intended as a product solicitation or promotion where such activities are prohibited. Because Hologic materials are distributed through websites, eBroadcasts and tradeshows, it is not always possible to control where such materials appear. For specific information on what products are available for sale in a particular country, please contact your local Hologic representative.

www.hologic.com | dxaperformance.com | 1.800.442.9892

Skeletal Biology and Disease Modeling in Zebrafish

Kristin Dietrich,^{1*} Imke AK Fiedler,^{2*} Anastasia Kurzyukova,^{1*} Alejandra C López-Delgado,^{1*} Lucy M McGowan,^{3*} Karina Geurtzen,¹ Chrissy L Hammond,³ Björn Busse,^{2,4} and Franziska Knopf¹

¹Center for Regenerative Therapies TU Dresden (CRTD), Center for Healthy Aging TU Dresden, Dresden, Germany

²Department of Osteology and Biomechanics, University Medical Center Hamburg-Eppendorf, Hamburg, Germany

³School of Physiology, Pharmacology and Neuroscience, University of Bristol, Bristol, UK

⁴Interdisciplinary Competence Center for Interface Research (ICIR), Hamburg, Germany

ABSTRACT

Zebrafish are teleosts (bony fish) that share with mammals a common ancestor belonging to the phylum Osteichthyes, from which their endoskeletal systems have been inherited. Indeed, teleosts and mammals have numerous genetically conserved features in terms of skeletal elements, ossification mechanisms, and bone matrix components in common. Yet differences related to bone morphology and function need to be considered when investigating zebrafish in skeletal research. In this review, we focus on zebrafish skeletal architecture with emphasis on the morphology of the vertebral column and associated anatomical structures. We provide an overview of the different ossification types and osseous cells in zebrafish and describe bone matrix composition at the microscopic tissue level with a focus on assessing mineralization. Processes of bone formation also strongly depend on loading in zebrafish, as we elaborate here. Furthermore, we illustrate the high regenerative capacity of zebrafish bones and present some of the technological advantages of using zebrafish as a model. We highlight zebrafish axial and fin skeleton patterning mechanisms, metabolic bone disease such as after immunosuppressive glucocorticoid treatment, as well as osteogenesis imperfecta (OI) and osteopetrosis research in zebrafish. We conclude with a view of why larval zebrafish xenografts are a powerful tool to study bone metastasis. © 2021 American Society for Bone and Mineral Research (ASBMR).

KEY WORDS: ZEBRAFISH; SKELETON; REGENERATION; METASTASIS; GLUCOCORTICOID

Introduction

Zebrafish have become an important model organism to study the development and disease of the skeleton in basic and pre-clinical research. The potential of these teleost fish lies in their small size, ease of care, genetic amenability, and high regenerative capacity. Moreover, thanks to the transparency of embryonic and larval stages, osteogenesis and osteoblast activity can be monitored in much detail, using available transgenic and mutant lines affecting specific cells or tissues.^(1,2) This is combined with long-term in vivo imaging feasibility of embryonic, larval, and also adult individuals,^(3,4) which distinguishes zebrafish from other vertebrate models such as rodents, in which intravital imaging can be challenging (Table 1). Importantly, the zebrafish genome contains orthologues of about 82% of human disease-related genes,⁽¹⁸⁾ including those affecting the skeleton. Both tissue-specific overexpression via site-specific recombinases (Cre)⁽³²⁾ and gene-specific knockout via clustered regularly interspaced short palindromic repeats (CRISPR)-Cas9⁽³⁰⁾ are available in zebrafish, along with antisense oligonucleotide gene knockdown approaches⁽³³⁾ and ideal conditions to carry out forward and reverse genetic screens.^(28,34,35)

Furthermore, single-nucleotide genome editing can be performed by CRISPR-Cas9-mediated knock-ins.^(36,37) Finally, drugs can be administered to zebrafish in various ways including dissolving chemicals directly in zebrafish water/media,^(11,38) the preferred method in drug screening (Table 1).

The above descriptions illustrate the potential of zebrafish to study skeletal biology and disease. Excellent reviews have been published on diverse aspects of zebrafish as a skeletal research model.^(39–42) Here, we aim to introduce zebrafish to the wider bone research community, by presenting essential information on their skeletal architecture and patterning, cell types, and matrix mineralization (which is loading dependent), along with introducing a variety of zebrafish assays to study bone regeneration. Furthermore, we highlight the utility of larval xenografts to demonstrate the power of zebrafish in bone metastasis research.

Architecture of the Zebrafish Skeleton

The skeleton of vertebrates is generally divided into the exoskeleton and endoskeleton.⁽⁴³⁾ The prominent parts of the zebrafish skeleton are as follows: (i) the craniofacial skeleton

Received in original form July 15, 2020; revised form January 15, 2021; accepted January 20, 2021; Accepted manuscript online January 23, 2021.

Address correspondence to: Björn Busse, PhD, Department of Osteology and Biomechanics, University Medical Center Hamburg-Eppendorf, Hamburg, Germany. E-mail: b.busse@uke.uni-hamburg.de and Franziska Knopf, PhD, CRTD - Center for Regenerative Therapies TU Dresden, Center for Healthy Aging TU Dresden, Germany. Email: franziska.knopf@tu-dresden.de

*KD, IAKF, AK, ACLD, and LMM contributed equally to this work.

Journal of Bone and Mineral Research, Vol. 00, No. 00, Month 2021, pp 1–23.

DOI: 10.1002/jbmr.4256

© 2021 American Society for Bone and Mineral Research (ASBMR)

Table 1. Comparison of Skeletal Features and Experimental Tractability in Humans, Rodents, and Zebrafish

Skeletal feature	Human	Rodent	Zebrafish	References
Bone types	Dermal Compact Spongy	Dermal Compact Spongy	Dermal Compact Tubular (spongy)	(5)
Skeletal cell types	Chondrocytes Osteoblasts Osteoclasts (multinucleate) Osteocytes	Chondrocytes Osteoblasts Osteoclasts (multinucleate) Osteocytes	Chondrocytes Osteoblasts Osteoclasts (multinucleate and mononucleate) Osteocytes	(5,6)
Ossification types	Endochondral Intramembranous Perichondral	Endochondral Intramembranous Perichondral	Endochondral Intramembranous Perichondral	(5,7)
Development	In utero	In utero	Extrauterine	
Average brood size	n/a	6–8	100–150	(8)
Mineralization begins	4–5 weeks	about 2 weeks	3–4 dpf	(9,10)
Skeletal maturity reached	Up to 30 years	4–5 months	2–4 months	(11)
Direction of loading	Axial	Orthogonal	Axial	(12)
Repair after fracture	Yes	Yes	Yes	(13,14)
Regeneration after amputation	Limited (digit tip)	Limited (digit tip)	Yes	(15–17)
Gene conservation (versus humans)	100%	~85%	~75%	(18)
Bone marrow	Yes	Yes	No	(19)
Dynamic histomorphometry	Tetracycline	Alizarin red stain Calcein green	Alizarin red stain Calcein green	(20–22)
Visualization of cell dynamics of bone	No	Limited (intravital imaging)	Transparency in mutants, larval stages and fin regenerates, adult scale regeneration	(4,15,23,24)
BMD assessment	CT (fixed/live); high- resolution peripheral quantitative CT (HRpQCT, fixed/live); ultrasound (live); DXA (live)	μCT (fixed); DXA (live)	μCT (fixed)	(25–27)
Drug screening	In vitro	In vitro	In vivo	(11)
Mosaic CRISPR mutagenesis time	n/a	3 months	5 days to 3 months	(28,29)
Stable CRISPR mutagenesis time	n/a	9 months	6–9 months	(30)
Ex vivo/in vitro study of bone	In vitro differentiation of stem cells Ex vivo culture of 1° cells	In vitro differentiation of stem cells Ex vivo culture of 1° cells	Ex vivo scale culture Ex vivo culture of 1° cells	(23,31)

1° = primary; n/a = not applicable; dpf = day(s) post fertilization.

including parietal bones, jaw bones, and opercles (bones covering the gills); and (ii) the axial skeleton comprising the vertebral column, ribs, intermuscular bones, as well as unpaired dorsal, anal, and caudal fins^(44,45) (Fig. 1A). Zebrafish are considered sexually mature at ~90 days, corresponding to a standard length (SL; measured from snout to the last caudal vertebra in adult individuals) of 1.5 to 2.0 cm. Zebrafish undergo continuous growth associated with an increase in skeletal volume, resulting in a body length of 3 to 4 cm, and

typically live for around 3 years (though they can reach 5 years).⁽⁴⁶⁾

The adult zebrafish skull is composed of 74 craniofacial bones, considerably more than the 22 bones of the mammalian skull.⁽⁴⁷⁾ Nevertheless, a number of bony structures in zebrafish have clear homologs in mammals, including the anterior part of the neurocranium, which resembles the mammalian palate,⁽⁴⁸⁾ and the cranial vault, which is conserved between zebrafish and mammals.⁽⁴⁹⁾ As with mammals, the zebrafish

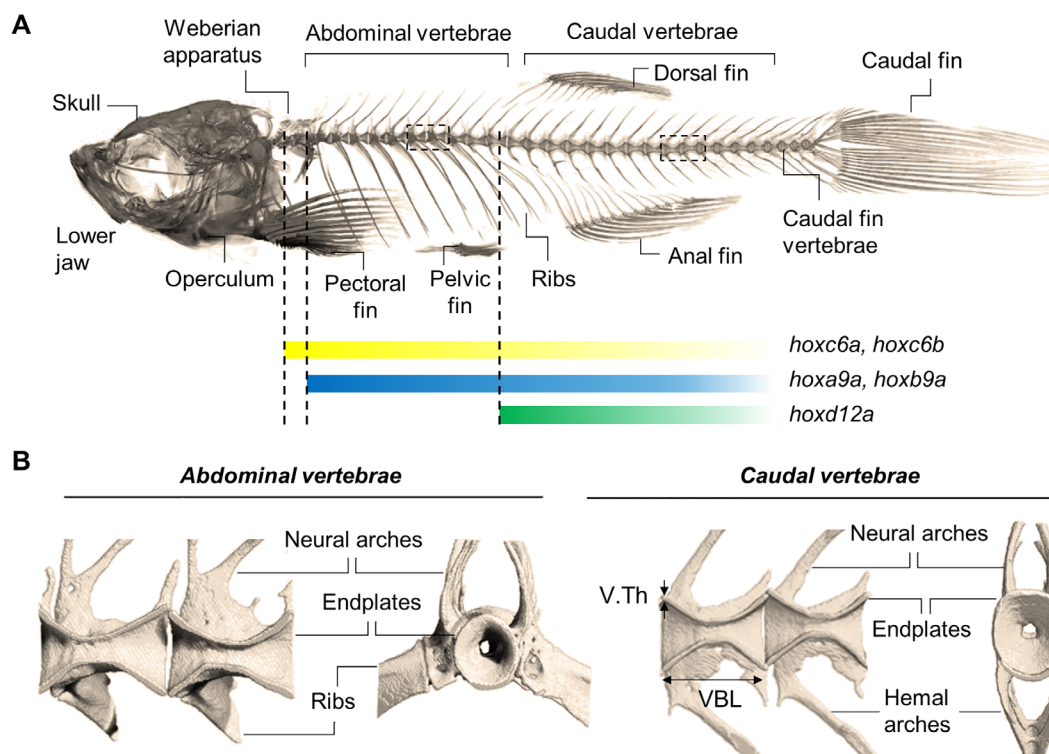


Fig 1. The zebrafish skeleton. (A) μ CT image of the craniofacial and axial skeleton, including the vertebral column composed of the Weberian apparatus, abdominal (also referred to as precaudal or thoracic), caudal, and caudal fin vertebrae. *Hox* gene expression patterns are indicated. Similar to the mammalian skeleton, ribs in zebrafish are articulated to the abdominal vertebrae and protect the inner organs. (B) Close-up view of abdominal and caudal vertebrae. Sagittal views of two adjacent double-cone shaped vertebrae (left) display the neural arches extending dorsally and encompassing the neural canal. Extending ventrally from the abdominal vertebrae ribs are articulated, while the caudal vertebrae extend to hemal arches which encompass the caudal artery and vein. In frontal view (right), the unmineralized vertebral center is revealed which contains notochord and vacuolated soft tissue (not displayed). The ring-shaped vertebral endplate regions are connected by an IVL (not shown) and correspond to the vertebral growth zone in zebrafish. Parameters, including the VBL, V.Th, and BV/TV, provide valuable measures to quantify the vertebral morphology and structure. BV/TV = bone volumetric fraction; IVL = intervertebral ligament; VBL = vertebral body length; V.Th = vertebral thickness.

skull features skeletal joints, including fibrous joints (eg, skull sutures), and articular joints in the jaw.⁽⁵⁰⁾

Regarding spinal morphology, zebrafish share a similar number of vertebrae (30 to 32 in zebrafish versus 33 in humans) and a physiological curvature with humans: kyphosis in the abdominal region where the ribs protect the viscera, and lordosis in the caudal region.⁽⁵¹⁾ In craniocaudal order, the zebrafish vertebral column is composed of a Weberian apparatus consisting of four vertebrae connecting the swim bladder to the ear (important for the transmission of sound), 10 abdominal vertebrae (also known as precaudal vertebrae or trunk vertebrae) that are articulated with rod-shaped rib segments, transitioning into 14 caudal vertebrae, and three caudal fin vertebrae.⁽⁵²⁾ (Fig. 1A). The spinal cord passes through the neural arches that extend dorsally from each vertebra, similarly to the mammalian spinal canal. Caudal vertebrae also have hemal arches that extend ventrally and enclose the caudal artery and vein.

The three-dimensional (3D) morphology of individual zebrafish vertebral body centra is characterized by its hourglass shape (Fig. 1B). In contrast to mammalian vertebrae that contain trabecular bone and carry bone marrow (BM), zebrafish vertebral bodies do not accommodate red BM, because adult hematopoiesis takes place in the kidney (Table 1). Instead, they are filled with

vacuolated notochord cells and become surrounded by adipose tissue.^(53,54) Micrometer-thin trabecular struts are found surrounding the narrow center of individual vertebrae.⁽⁵⁾

Although assessment of vertebral trabecular bone, a readout for bone fragility in mammals, is limited in zebrafish, morphology of the vertebral centra is commonly used as an indicator for vertebral bone quality. 3D morphometric parameters, eg, vertebral body length (VBL), bone volume (BV), bone volume per tissue volume (BV/TV), vertebral cross-sectional thickness (V.Th), and eccentricity (ie, roundness) are extracted from micro-computed tomography (μ CT) scans of the zebrafish spine (Fig. 1B), allowing the quantification of changes, eg, due to altered musculoskeletal activity,^(55,56) aging,⁽⁵⁷⁾ and disease.⁽⁵⁸⁾ In addition, thickness and volume of hemal and neural arches are used to assess vertebral morphology in zebrafish mutants.⁽²⁵⁾ One advantage of the small-sized zebrafish is the possibility of analyzing the complete skeleton at high resolution (eg, a whole-body μ CT scan at a pixel size of $1 \mu\text{m}^2$), more rapidly than it is possible in larger rodent species. This provides the possibility to both evaluate the bulk 3D morphology of the entire organism and to simultaneously characterize tissue morphology at high resolution,⁽⁵⁹⁾ which has been done in deformed osteoarthritic vertebral bodies.⁽⁶⁰⁾ Furthermore, longitudinal histological sections or whole-mount

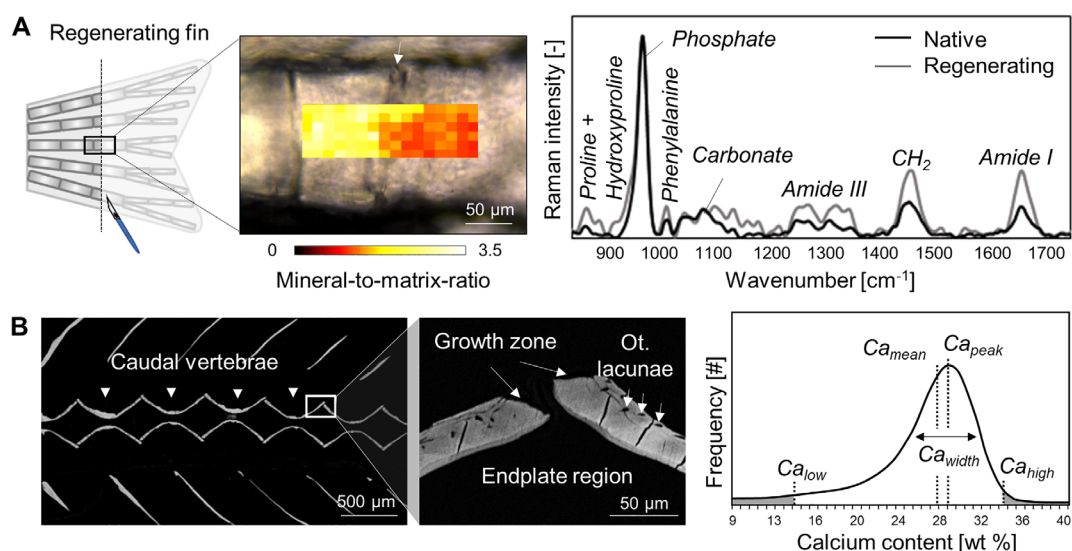


Fig 2. Assessment of matrix composition in zebrafish bone. (A) Raman spectroscopy allows mapping the mineral-related and protein-related properties of regenerating caudal fin bone (here, mineral-to-matrix ratio at 7 dpa) proximal and distal to the amputation plane (arrow). In the Raman spectra of regenerating parts (gray curve), protein-related peaks including amide I, amide III, and hydroxyproline, are more pronounced in respect to the mineral-related phosphate peak, reflecting a lower mineral-to-matrix ratio compared to native bone tissue (black curve). (B) qBEI can be used to assess the mineral density distribution in the zebrafish skeleton (here: sagittal plane of the vertebral column and close-up of the endplate region). A histogram generated from calibrated pixel intensities within a region of interest allows extracting the Ca_{mean} , Ca_{peak} , and Ca_{width} , as well as areas with Ca_{low} and Ca_{high} . Ca_{high} = high degree of mineralization; Ca_{low} = low degree of mineralization; Ca_{mean} = mean Ca content; Ca_{peak} = peak Ca content; Ca_{width} = heterogeneity of the Ca distribution; dpa = days post amputation; qBEI = quantitative backscattered electron microscopy.

stains, eg, Alizarin red staining, enable the display of the complete skeleton at microscopic resolution.^(20,45,61)

Similar to mammals, vertebral bones in zebrafish are interconnected by soft tissue, facilitating movement and increasing the range of locomotion. In mammals, the intervertebral disk (IVD) is composed of fibrocartilaginous cartilage (annulus fibrosus) and nucleus pulposus. In contrast, the intervertebral soft tissue in zebrafish is characterized by a ring-shaped ligament (intervertebral ligament [IVL]) connecting the outermost circular edges of two adjacent vertebrae. Although the physiological role of the IVD in humans is damping compressive forces from gravitational loading, the zebrafish spine is loaded axially due to compressive forces from swimming through viscous water and direct muscle forces transmitted by tendons attached to the vertebrae.⁽¹²⁾ Compared to tetrapods (eg, mice, dogs), where gravitational forces apply orthogonally to the spine, zebrafish can be considered advantageous in terms of loading regime. Thus, they provide a valuable tool to study spine and intervertebral tissue degeneration and effects of altered locomotion patterns on the bone-tendon-muscle unit, which can be assessed in small-sized zebrafish using histological and advanced X-ray imaging approaches⁽⁶²⁾ (Fig. 2).

Patterning of the Zebrafish Axial and Fin Skeleton

As in other vertebrates, axial patterning in the zebrafish skeleton manifests in the vertebral column which is regionalized into different types of vertebrae along the anteroposterior axis.⁽⁵²⁾ Studies in mice and chicken revealed the morphological diversity and

axial position of the different types of vertebrae that are sensitive to positional cues encoded by regional *Hox* gene expression.^(63,64) Although HOX mutations in humans lead to early developmental lethality, HOX-related axial skeletal defects have been described, in addition to limb and craniofacial defects, arthritis, and diverse types of cancer.^(65,66) Regionalization of the zebrafish axial skeleton is under the same mechanistic control, and relies on spatial (and temporal) collinearity; ie, the correspondence between the physical sequence of the genes on the chromosome and their anteroposterior boundaries (and timing) of expression^(63,67) (Fig. 1A). Although there are 39 *Hox* genes distributed in four clusters in the mammalian genome, zebrafish possess 48 genes in seven clusters. These differences have come about as a result of genome duplication and gene loss during vertebrate evolution.^(68,69) Accordingly, *Hox* expression domains and axial structure regionalization are only partially equivalent between zebrafish and tetrapods (true, eg, for *Hoxc6* and *Hoxd12* but not for *Hox9*).^(64,67,70) Nevertheless, studying homeotic transformations in embryonic and larval zebrafish may be a useful tool to reveal the variety of *Hox* protein regulatory functions.

In fish, the axial skeleton includes the vertebral column and associated median fins (dorsal, anal, and caudal), whereas the paired pectoral and pelvic fins are located ventrolaterally in the abdominal region. Positioning of the dorsal and anal fin has not been investigated in zebrafish, but hypothetically may be determined as in sharks by the expression domain of *Hox* and *Tbx* genes.⁽⁷¹⁾ The development of the pectoral fin shows high similarity with tetrapod limb development especially at early stages, regarding *Hox* expression^(72–74) and inductive signals such as retinoic acid (RA)^(75–78) (Fig. 3A–F). During gastrulation, RA is responsible for limb field positioning.⁽⁷⁹⁾ Subsequently, RA

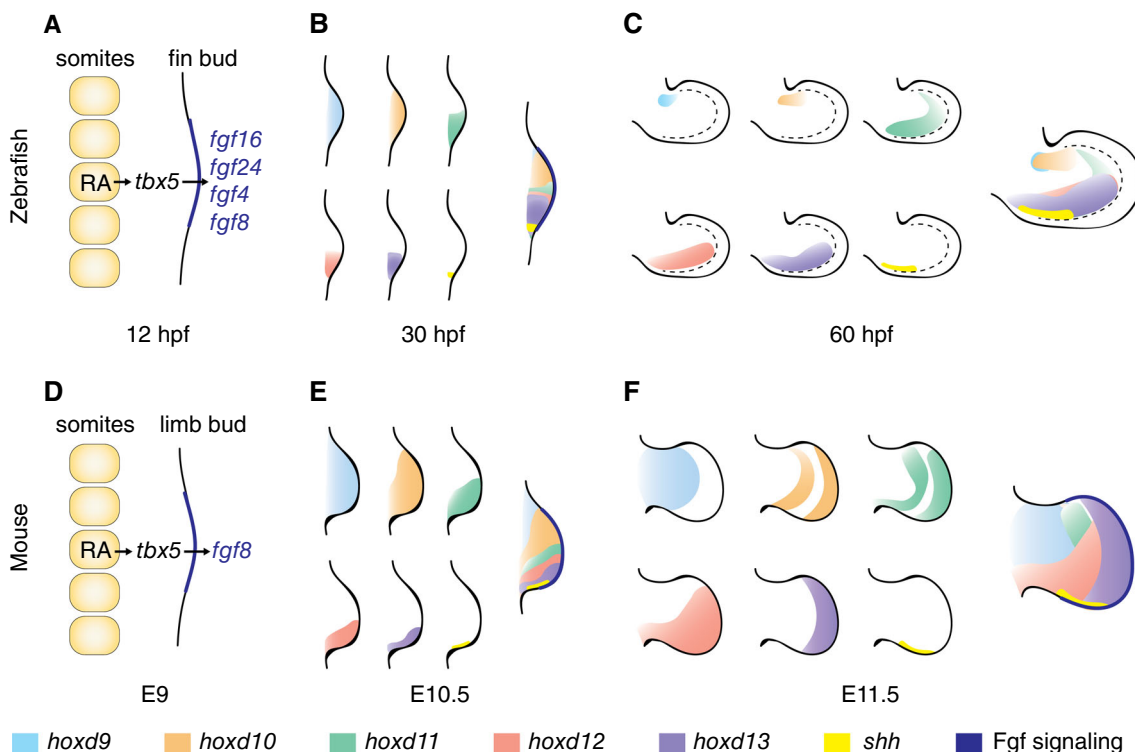


Fig 3. Early patterning of limb and pectoral fin buds is comparable. (A–C) Early zebrafish fin bud patterning. (A) Fin induction at 12 hpf: RA from the somites activates signals that lead to activation of *tbx5* in the lateral plate and Fgf signaling in the distal bud, establishing the AER. (B) Early expression of *Hox* genes and *shh* at 30 hpf. (C) Expression of *Hox* genes and *shh* at 60 hpf. Note that the *hoxd11* expression domain in the posterior fin bud region remains restricted to this region at 30 hpf and 60 hpf. Dashed line = boundary of fin bud proper and fin fold. (D–F) Early mouse limb bud patterning. (D) Similar induction signals as described in A for the fin bud occur in the mouse at E9. (E) Early expression of *Hox* genes and *shh* in E10.5 mouse limbs shows a similar pattern observed as in B for the fin bud. While *hoxd9* and *hoxd10* extend through the whole bud, *hoxd11*, *hoxd12*, *hoxd13*, and *shh* are restricted to the posterior domain. (F) *Hox* expression domain in E12.5 mouse limbs differs from those observed in C in the fin bud; *hoxd11*, *hoxd12*, and *hoxd13* domains extend more anteriorly; and *shh* remains restricted to the posterior region. Left to right = proximodistal axis, top down = anterior–posterior axis. E10.5 = embryonic day 10.5; E12.5 = embryonic day 12.5; E9 = embryonic day 9; hpf = hours post fertilization.

is produced in somites and activates Wnt2b⁽⁷⁸⁾ in the intermediate mesoderm, which in turn activates *Tbx5* in the lateral plate mesoderm.^(77,78) *Tbx5*, the earliest transcription factor in forelimb initiation, then triggers fibroblast growth factor (Fgf) signaling, establishing a transcriptional cascade regulating proximodistal patterning of the appendage. Both in tetrapods and fish, two signaling organizers are formed in the anlage of the appendage: the apical ectodermal ridge (AER) in the distal bud, which regulates limb and fin outgrowth through Fgf signaling,^(75,78) and the zone of polarizing activity (ZPA) that is marked by posterior expression of *sonic hedgehog* (*shh*) and regulates anteroposterior patterning.^(72,77,80) The non-ridge ectoderm instructs dorsoventral patterning.⁽⁸¹⁾ Although the mechanisms are apparently conserved, differences in regulation and patterning of the fin and limb at later stages suggest that expression patterns and signaling mechanisms have been modified during evolution, ie, during fin to limb transition, which may have led to the generation of novel skeletal features such as tetrapod digits.⁽⁸²⁾ Side by side comparison of *Hox* gene expression and modulation of these and other patterning determinants in tetrapods and fish including zebrafish will uncover more aspects of skeletal evolution and congenital patterning defects in humans in the future.

Types of Ossification and Osseous Cells

In zebrafish, ossification first occurs 3 to 4 days post fertilization (dpf), progressively leading to the formation of a mature skeleton by 2 to 4 months (dependent on zebrafish size, Table 1). Many elements form by intramembranous and perichondral ossification, with some elements formed by endochondral ossification⁽⁵⁾ (Table 1). Depending on the anatomical region, the zebrafish skeleton is formed by either of the three ossification types.⁽⁷⁾ Intramembranous ossification is the major form of ossification in the zebrafish skeleton and occurs in elements such as the cranial roof, the opercles covering the gills, and most vertebrae.⁽⁷⁾ Endochondral ossification, in which a cartilage template is successively replaced by bone, gives rise to only a few elements including the neural arches of vertebrae 1 to 5.⁽⁵⁾ Perichondral ossification occurs on a chondral surface without replacing the cartilage template, and takes place in the lower zebrafish jaw. Although mammalian vertebrae exclusively form via a cartilage intermediate, zebrafish centrae, directly mineralize from the notochord sheath, an ossification layer around the notochord, followed by intramembranous bone formation.⁽⁸³⁾ Notably, the notochord sheath is also responsible for segmentation of the zebrafish spine prior to centra formation.⁽⁸⁴⁾

Based on the evolutionary conservation of skeletal genes across vertebrates, zebrafish bone contains the same osseous cells that are found in mammals, namely osteoblasts, osteoclasts, and osteocytes (Table 1). Like in mammals, bone apposition is performed by osteoblasts derived from osteoprogenitor cells. In the zebrafish skeleton, a large fraction of bone surface is covered by osteoblasts, whose morphology can vary greatly and is dependent on their location and function.⁽⁵⁾ In the spine, osteoblastic bone formation leads to an increase in vertebral volume and length in anterior and posterior directions, which elongates the spine. This bone formation can be assessed easily in the intervertebral growth region, more specifically on the circular vertebral body endplates⁽⁸⁵⁾ (Fig. 1B). Bone can be analyzed in the zebrafish spine by using the static histomorphometry protocols that are commonly applied to rodent bones or human biopsies, including the number of osteoblasts per bone perimeter (N. Ob/B.Pm), osteoid surface per bone surface (OS/BS), and osteoid thickness (O.Th).^(56,58) However, zebrafish bone can also be labeled with fluorescent dyes like calcein or Alizarin red at consecutive time points, providing the opportunity to perform dynamic histomorphometry and determine the bone formation rate (BFR) and bone mineral apposition rate (MAR)^(56,58) (Table 1). In contrast to rodent models or humans, where dyes are applied by injection or ingestion, zebrafish are more commonly stained by bathing them in the dye solution.

Bone resorption in zebrafish is performed by mononucleated and multinucleated osteoclasts. Although mononucleated osteoclasts are present at the early stages of development and are associated with shallow resorption patterns, multinucleated osteoclasts create resorption lacunae typically described for mammalian osteoclasts later in life.⁽⁶⁾ Similar to mammals, both types of osteoclasts express tartrate-resistant acid phosphatase (TRAP).^(6,86)

Concepts of bone modeling and remodeling described for mammalian bone can also be applied to zebrafish. While bone modeling is defined as the process of adapting bone shape by bone formation and resorption in response to increased or reduced loading at different surfaces, remodeling is carried out in the same location to maintain bone matrix quality and to repair microcracks.⁽⁵⁶⁾ Remodeling, which involves the orchestration of both osteoclasts and osteoblasts by mechanosensitive osteocytes to renew bone and repair microcracks, is less pronounced in zebrafish. Osteons are essentially not present. Yet remodeling processes in zebrafish are suggested to occur site-dependently and to be linked to the demand of lifelong growth.⁽⁶⁾

Zebrafish bone, in contrast to bone of the medaka fish (*Oryzias latipes*, another teleost), is generally osteocytic, although the vertebral bones do not contain osteocytes in early juvenile stages and the bony fin rays and scales remain anosteocytic throughout life.⁽⁸⁷⁾ Although mammalian osteocytes are the main orchestrator of remodeling, only a few studies have focused on the mechanosensing capabilities of the osteocyte lacunar network and dendrite characteristics in zebrafish. There is, however, evidence for a relationship between the morphology of the osteocyte network and bone formation in a zebrafish Ol model, in which altered bone formation is associated with drastically reduced numbers of osteocyte lacunae.⁽⁵⁸⁾ This information illustrates some important differences but also many commonalities between zebrafish and mammalian bone biology (Table 1).

Bone Matrix and Mineralization in Zebrafish

Vertebrate bone is composed of a soft matrix containing mainly collagen I and noncollagenous proteins and hardens by

incorporation of carbonated bone apatite. Although the degree of mineralization varies among vertebrate species, the basic macromolecular and elemental composition of bone matrix is conserved between mammals and zebrafish. The presence of phosphate, carbonate, amide I and III, proline, hydroxyproline, and phenylalanine in zebrafish bone has been demonstrated with vibrational spectroscopy.^(58,88–91) These analyses have shown the typical fingerprints of collagenous matrix with embedded carbonated bone apatite. In growing fin bone, amorphous calcium phosphate is suggested to transform into more crystalline mineral during tissue maturation.⁽⁸⁸⁾ In addition to calcium (Ca) and phosphorous (P), magnesium is one of the main minerals stored in zebrafish bone.⁽⁹²⁾ Moreover, trace elements including strontium and zinc are involved in bone formation, similar to the mammalian situation. In particular, these elements have been detected in scales⁽⁹³⁾ and vertebral bone matrix⁽⁹⁴⁾ using X-ray fluorescence microscopy and energy dispersive X-ray spectroscopy, respectively.

Clearly, some differences apply in terms of mineral metabolism between teleosts and terrestrial mammals. In contrast to tetrapods, which depend on both dietary P and Ca intake for maintaining the Ca-P-based bone matrix, zebrafish live in a Ca-rich environment and absorb Ca through their gills. However, dietary P intake is required, and reducing the P levels either through genetic manipulation or through a reduced diet leads to nonmineralizing matrix.^(95,96)

As in mammals, the composition and organization of the bone matrix is crucial to providing fracture resistance in zebrafish. Specifically, the sum of collagen-related and mineral-related structural properties (collagen alignment, enzymatic and nonenzymatic crosslinking, size and orientation of mineral particles) and compositional properties (carbonate-to-phosphate ratio), as well as the degree of mineralization in terms of overall bone mineral density (BMD) or local Ca content and distribution, determine the mechanical properties at the tissue level. This translates into fracture risk at the whole bone level.^(58,94) Several techniques have been adapted from mammalian bone analyses to determine the degree of mineralization in micrometer-sized zebrafish bone (Table 1). μ CT based on calibration with hydroxyapatite phantoms has been used to assess BMD in the spine of zebrafish.⁽²⁵⁾ Indeed, variations in BMD due to mutations support the presence of similar mineralization pathways in zebrafish and mammalian models. The macromolecular composition of pathologic bone matrix in zebrafish carrying mutations in *coll1a1* has been analyzed by vibrational spectroscopy and demonstrated alterations in the mineral-to-matrix and carbonate-to-phosphate ratios.⁽⁵⁸⁾ Moreover, remineralization in regenerating zebrafish fin bones after amputation can be monitored using vibrational spectroscopy, allowing the comparison of new bone quality with the quality of native bone (Fig. 2A). Another indicator for a well-mineralized bone matrix is the Ca content and the distribution of Ca within the bone matrix. These parameters are commonly assessed in rodents and human biopsies using two-dimensional (2D) quantitative-backscattered electron microscopy (qBEI)⁽⁹⁷⁾ (Fig. 2B). More recently, qBEI has also been adapted to zebrafish vertebral bone, in which an increase in mean Ca content by ~8% has been linked to increased musculoskeletal activity.⁽⁵⁶⁾

Increased mineralization may lead to increased bone fracture resistance.^(98,99) Although whole-bone mechanical testing of zebrafish bones, eg, of individual vertebrae, is challenging (though possible)⁽¹²⁾ due to their small size (VBL = 500 μ m), nanoindentation techniques are valuable tools to assess mechanical properties of zebrafish vertebral bone at the tissue level. As an example, rising Ca/P ratios have been associated with

an increase in elastic modulus in zebrafish vertebral bone during aging.⁽⁹⁴⁾ However, the opposite effect can be observed as well. In case of disturbed collagen and consecutive mineral particle deposition (eg, in *chihuahua*,⁽⁵⁸⁾ *liliput*,⁽⁹¹⁾ and *stöpsel*⁽¹⁰⁰⁾ zebrafish mutants), the elastic modulus of vertebral bone is reduced despite a higher degree of mineralization, stressing the importance of well-organized matrix mineralization to withstand fracture. Notably, zebrafish bone matrix elastic modulus values lie in a similar range as in mammals (up to 24 GPa),⁽¹⁰¹⁾ highlighting the similarities in bone matrix composition and mechanical properties between both. This substantiates the use of zebrafish as a model to study the effects of genetic alterations and external stimuli on bone matrix quality.

Problems in matrix mineralization such as those present in phosphate homeostasis disorders have been phenocopied in zebrafish. Phosphate is an essential mineral for hydroxyapatite formation in bone,⁽¹⁰²⁾ and its lack (hypophosphatemia) is provoked in mutants, in which essential genes for phosphate regulation are altered. The *no bone* (*nob*) mutant, in which the gene *ectonucleoside triphosphate diphosphohydrolase 5* (*entpd5*) is affected, forms no mineralized bone at all.⁽¹⁰³⁾ In another mutant, *dragonfish* (*dgf*), the gene *ectonucleotide pyrophosphatase/phosphodiesterase 1* (*enpp1*) is mutated, leading to reduced pyrophosphate levels and ectopic mineralization of the axial and craniofacial skeleton.⁽¹⁰³⁾ The *dgf* mutant shows altered expression of genes related to phosphate homeostasis and bone mineralization, such as *fgf23*, *solute carrier family 34 member 1a* (*slc34a1a*, also known as *npt2a*), *entpd5*, and *secreted phosphoprotein 1* (*spp1*), and can thus also be used to model generalized arterial calcification of infancy (GACI) and pseudoxanthoma elasticum (PXE).⁽¹⁰⁴⁾ Restored skeletal mineralization is observed in double mutant *nob/dgf* zebrafish, indicating a reciprocal regulation of *Entpd5* and *Enpp1*.⁽¹⁰⁴⁾ This illustrates the usefulness of zebrafish mutant analyses and state-of-the-art technology to understand mineralization defects in vertebrates.

Response of the Zebrafish Skeleton to Loading

Although loading of the zebrafish skeleton differs from that of terrestrial animals, due to the supportive buoyancy of water, the skeleton does respond to mechanical loading (Table 1). This comes from the action of muscle contraction on the skeleton, and reaction forces from swimming through a viscous medium.

During early fetal life all vertebrates develop in an aqueous environment, whether in utero, in ovo, or in water (Table 1). During this time, biomechanical stimuli acting on the developing skeleton are caused by the action of muscle on skeletal tissues.⁽¹⁰⁵⁾ It has been demonstrated in mice, chicks, and humans that restriction of fetal movement leads to altered mineralization and to failure of joint and eminence morphogenesis.^(106–108) In zebrafish, genetically or pharmacologically induced paralysis leads to altered chondrocyte maturation⁽¹⁰⁹⁾ and abnormal joint morphogenesis through changes in chondrocyte proliferation and migration.^(110,111) Finite element (FE) modeling of the larval jaw, in which the structure is subdivided into smaller and simpler entities, allows modeling of the loading effects on tissue deformation, and has demonstrated that altered joint shape impacts the pattern of biomechanical strain.^(112,113) It is well established that biomechanical loading of the joint is a key risk factor for osteoarthritis. Moreover, mutants such as *col11a2* and *prg4* exhibiting altered joint shape go on to develop osteoarthritis in these joints.^(50,113,114) Given the recent identification of loci associated

both with osteoarthritis and altered joint shape in presymptomatic humans^(115,116) and the need for functional screening platforms, this raises the prospect of using zebrafish to screen for osteoarthritis susceptibility genes implicated in joint development and maintenance (Fig. 4).

Mineralization of the vertebral column and fins of zebrafish occurs much later than the onset of locomotion, with first mineralization of vertebral centra observed at around 7 dpf (SL = 3.8 mm), and vertebral arches and fin rays at around day 14 (SL = 5–6 mm).^(52,117) Vertebral bone formation can be triggered by increased physiological musculoskeletal loading in adult zebrafish, demonstrating that zebrafish bone is susceptible to positive bone modeling according to Wolf's law.⁽⁵⁶⁾ Zebrafish subjected to swim training for 9 hours a day from 5 to 14 dpf exhibit premature ossification of fin and vertebral column bone.⁽¹¹⁸⁾ In terrestrial species osteocytes function as mechanosensors, directing the remodeling activity of osteoblasts and osteoclasts, through the regulation of the glycoprotein Sclerostin (SOST).⁽¹¹⁹⁾ However, anosteocytic fish also model bone in response to load.⁽¹²⁰⁾ Swim training of osteocytic zebrafish and anosteocytic medaka led to strikingly similar patterns of new bone formation in both species, mediated by *sost* expression by chondrocytes and osteoblasts in regions of high strain modeled by FE on individual vertebrae.⁽¹²¹⁾ Interestingly, zebrafish vertebral motion analysis together with FE predict patterns of bone failure during loading,⁽¹²⁾ which could be used to test bone performance in mutants.

Gravity plays an important role in the loading of the skeleton of terrestrial animals, and prolonged exposure to microgravity (weightlessness or gravity close to zero) leads to decreased bone density in humans.⁽¹²²⁾ Perhaps surprisingly, gravity also impacts the skeleton of teleost fish. Several studies on medaka have been performed using an aquatic habitat on the International Space Station (ISS). These have demonstrated that medaka lose bone density following exposure to microgravity, show transcriptional changes to skeletal genes⁽¹²³⁾ and increased osteoclast activity.⁽¹²⁴⁾ Although zebrafish have not been reared on the ISS, they have been exposed to increased gravitational forces (hypergravity). Exposure to 3g to 9g during zebrafish larval development led to altered chondrocyte maturation⁽¹²⁵⁾ and changes to mineralization and the transcription of skeletal genes.⁽¹²⁶⁾ These studies illustrate the versatility of zebrafish models to study loading effects on bone.

OI and Osteopetrosis

The use of genetic tools, bone imaging, and pharmacological treatments in zebrafish models has increased our understanding of the pathophysiology of congenital skeletal diseases, and has been reviewed in detail.⁽³⁹⁾ OI is the term given to a collection of rare genetic bone collagenopathies, which are characterized by suboptimal skeletal development, aberrant bone architecture, and high fracture incidence.⁽¹²⁷⁾ There are multiple subtypes of OI, with varying degrees of severity; type I OI is the mildest form, which is underpinned by reduced production of normal type 1 collagen, whereas other types are the result of mutations which alter the molecular structure of type 1 collagen.⁽¹²⁸⁾ The majority of OI cases result from mutations in *COL1A1/A2*. The *chihuahua* zebrafish mutant, identified through forward genetic screening, was the first of several lines to accurately model OI in zebrafish.^(45,129) Heterozygous *chihuahua* zebrafish possess a dominant mutation in *col1a1*, resulting in gross

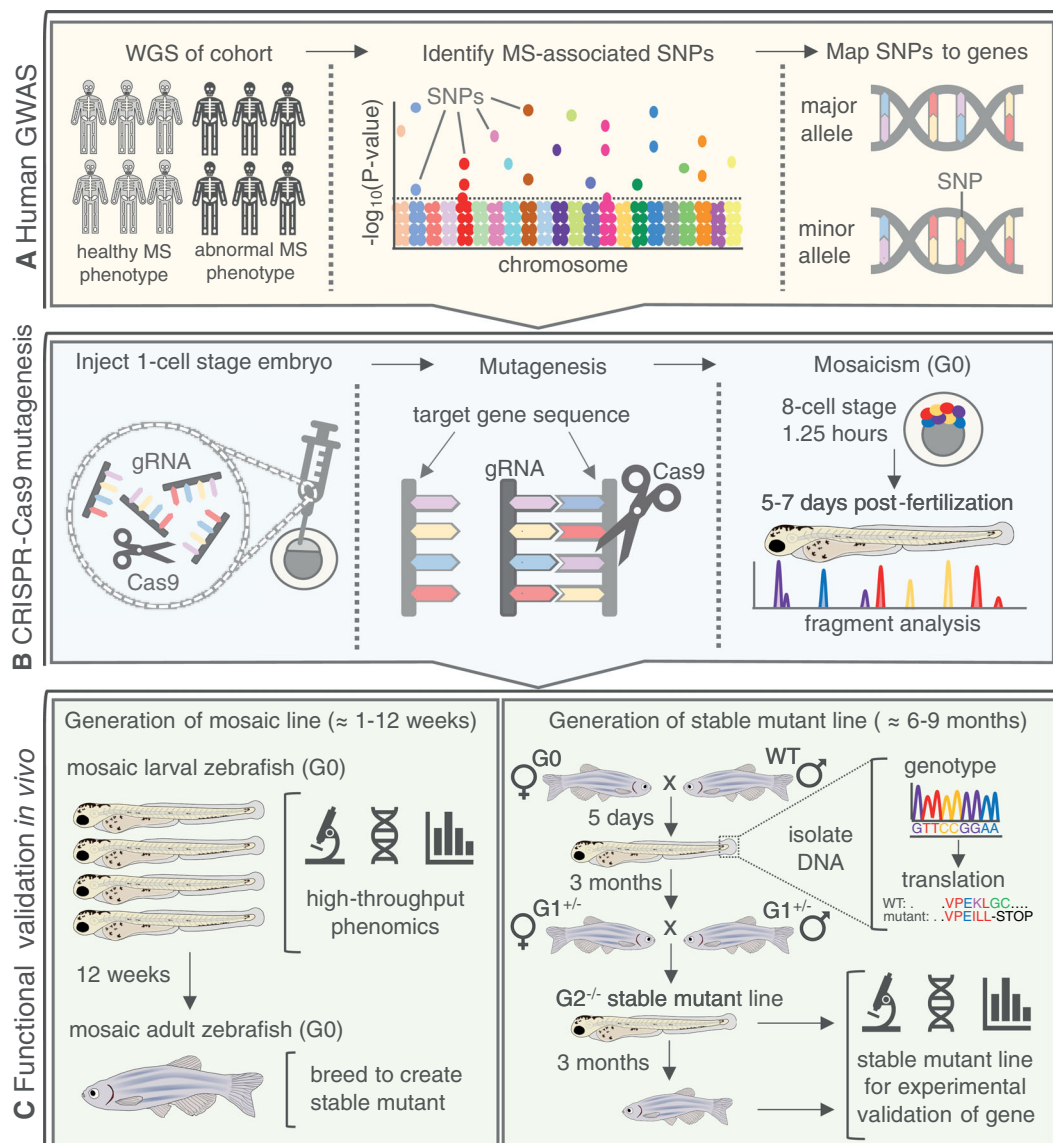


Fig 4. Zebrafish as a tool for rapid validation of GWAS-derived MS disease-associated gene candidates. (A) Human GWAS conduct WGS on large cohorts and identify SNP mutations in people with abnormal MS phenotypes. SNPs are then mapped to the nearest gene using whole-exome sequencing. (B) CRISPR-Cas9 technology can be used for targeted knockout mutagenesis in vivo. Gene-specific gRNAs are designed and injected into a one-cell stage zebrafish embryo with Cas9. Efficient gRNAs will facilitate double-strand breaks within an exon in the target gene, resulting in indel mutations. A mosaic (G0) embryo (crisprant) will develop, containing a variety of mutant and WT alleles for the gene of interest that are validated through fragment analysis. (C) (Left) mosaic larval zebrafish can be rapidly screened for MS phenotypes during skeletogenesis, providing a high-throughput and efficient phenomics-based approach to gene validation. Mosaic G0 zebrafish can be raised to adulthood for breeding into a stable line with a single, known mutant allele. (Right) G0 mosaic zebrafish are crossed to WT. Resulting heterozygous larvae (G1^{+/−}) are fin-clipped to isolate DNA for genotyping and in silico translation to identify alleles resulting in a premature STOP codon, compromising the protein. G1^{+/−} with the same mutant allele are bred with each other to generate the G2^{−/−} line with a stable mutation in the gene of interest. The stable mutant larvae or adults can then be used for experimental validation of the MS-associated phenotype. gRNA = guide RNA; hpf = hours post fertilization; MS = musculoskeletal; SNP = single-nucleotide polymorphism; WGS = whole-genome sequencing; WT = wild-type.

skeletal deformities and molecular abnormalities in bone mineralization OI.^(58,130) Some rarer forms of OI arise from mutations in collagen-processing genes such as *BMP1*, *PLOD2*, *CRTAP*, and *P3H1*,^(131–136) or osteoblast-related genes such as *SP7*,^(137,138) for which there are stable zebrafish mutant lines.^(139–142) Although there is no cure for OI, many patients are administered antiresorptive bisphosphonate drugs to increase BMD. Zebrafish

have been used to explore the role of bisphosphonates on bone in OI. For example, sustained treatment of the *frilly fins* (*bmp1a*) mutant with alendronate reduced the frequency of fractures in caudal lepidotrichia but could not rescue defects in fracture repair post injury.⁽¹⁴³⁾

At the opposite end of the spectrum, genes associated with high bone mass (osteopetrosis) have been modeled in

zebrafish. The *panther* (*csf1ra*) mutant zebrafish line exhibits low levels of osteoclast activity and osteopetrosis, due to the lack of colony stimulating factor 1 receptor α , which promotes the differentiation of myeloid lineage cells.^(144,145) Studies of the *panther* zebrafish line have helped to demonstrate the need for effective intercellular signaling by osteoblasts and osteoclasts throughout skeletal development and for maintaining bone architecture.^(143,144,146) More recently, integrative studies have used pedigree analyses to identify rare mutations in high bone mass genes such as *CLCN7* and *SMAD9*, followed by functional validation in zebrafish.^(11,147,148) Collectively, these studies have implicated the CIC-7/CTSK/TGF- β /SMAD (CHLORIDE ION CHANNEL 7/CATHEPSIN K/TRANSFORMING GROWTH FACTOR β /SMAD) signaling axis in osteopetrosis.

Human epidemiological analyses and genomewide association studies (GWAS) continue to rapidly identify new loci associated with skeletal health (Fig. 4A),^(149,150) yet these gene candidates require functional validation. In order to keep up with this pace, follow-up studies using zebrafish have evolved away from traditional forward genetic screening methods and toward modern genome editing tools such as CRISPR-Cas9 (Fig. 4B).⁽¹⁵¹⁾ Emerging phenomics-based deletion approaches in mosaic zebrafish (crispants) now present an efficient model for the rapid validation of novel GWAS-derived genes related to bone disease^(29,40) (Fig. 4B, C, Table 1). In many cases generating knockouts by the creation of indels with CRISPR-Cas9 can be informative, providing information on the nature of the putative associated genes and the likelihood that they are indeed causal. A potential limitation is reached when knock-in of the specific genetic change(s) identified in humans is required, because gene editing using homologous recombination or base editing, while possible,^(152–154) is less efficient than the generation of frameshift alleles through non-homologous end joining. Although stable mutant line generation by CRISPR-Cas9 knockin^(36,37) will be the gold standard to prove altered function of a gene due to a point mutation, mosaic deletion in crispants will be one of the ways to deal with the rich information obtained from GWAS.

The Regenerative Capacity of the Zebrafish Skeleton

Zebrafish regenerate various organs such as the retina, brain, heart, and pancreas, which has promoted the use of zebrafish as a regeneration model.⁽¹⁵⁵⁾ In teleosts and mammals, derivatives of dermal skeletal tissue are represented in terms of teeth, whereas endoskeletal tissue is represented in terms of bone and cartilage. In contrast to mammals, however, the dermal skeleton of zebrafish also encompasses fin rays and scales, which have the capability to regenerate throughout life⁽⁸⁷⁾ (Table 1). The presence of such tissues facilitates the study of skeletal features that do not exist in humans, including continuous tooth replacement,^(156,157) and regeneration of scales^(158,159) and fins.⁽¹⁵⁾ Moreover, calvaria and jaw bone regenerate in zebrafish (Fig. 5A–E, Table 2).

Zebrafish fins quickly and completely regenerate after profound amputation, a process which is regulated by various intercellular signaling pathway events.⁽¹⁷³⁾ In fact, regenerated fins are nearly indistinguishable from uninjured fins, as long as the endoskeletal elements (eg, hypurals) are retained during the amputation procedure.^(5,174–176) Notably, regenerative capacity of the caudal fin is not altered even after repeated

amputations.⁽¹⁷⁷⁾ The skeleton of the nonmuscular part of the caudal fin, predominantly used for regeneration studies because of its accessibility, is of dermal origin. The most prominent feature of this part is the presence of segmented bony fin rays (lepidotrichia), arranged in two concave hemirays. Bony fin rays contain loose mesenchyme (intra-ray fibroblasts), arteries and nerves and are covered by a sheet of osteoblasts and overlying epidermis. Inter-ray mesenchyme connects individual bony fin rays to each other.

Control over lepidotrichia segment length and joint formation, which significantly differs from endoskeletal joint formation, is crucial in regulating fin growth and regeneration. Although *gdf5*, an endoskeletal joint marker, is not expressed in lepidotrichia segment joints,^(178–180) distinct lepidotrichial joint markers such as *evx1* and the gap junction gene *cx43* have been identified.^(180,181) Notably, joint formation and segment length are regulated independently during growth of the fin.⁽¹⁸²⁾ Mutation of *cx43* leads to the *sof* (short fin) phenotype resulting from shorter fin ray segments due to an increased rate of joint formation.^(182,183) In contrast, longer fins in *long fin* (*lof*) and *rapunzel* mutants display normal-length segments, but more in number.^(182,184) In *another long fin* (*alf*) mutants with altered potassium channel function fins are longer and segment length is variable.⁽¹⁸⁵⁾ These phenotypes are reestablished during regeneration after fin amputation. We direct the interested reader to excellent expert reviews on this topic.^(41,186)

Regeneration occurs in a series of events. After amputation, epithelial cells at the wound site migrate to form a multilayered epithelium termed the wound epidermis.⁽¹⁸⁷⁾ Subsequently, mesenchymal cells from the stump migrate distally and proliferate to form the blastema,⁽¹⁸⁸⁾ which is a mass of cells restoring the missing structures. The blastema matures and subdivides into a distal signaling center (the most distal blastema),^(189,190) and a more proximal, highly proliferative growth and patterning zone.⁽¹⁹¹⁾ When blastemal organization is complete, regenerative outgrowth proceeds for approximately 2 weeks at high speed by coordinated cell proliferation and differentiation along the proximodistal axis, and is followed by slower growth until completion after 3 to 4 weeks post amputation depending on the amputation level.^(192,193)

The bony fin rays are the stabilizing elements of the fins and much progress has recently been made in describing their regeneration. During blastema formation, mature osteoblasts lining the inner and outer surface of the stump hemirays dedifferentiate by losing *bglap* (*osteocalcin*) and *sp7* (*osterix*) expression, a process that is regulated by RA and NF- κ B signaling.^(194,195) They migrate distally to form part of the blastema, where they then upregulate the immature osteoblast marker *runx2*. This is followed by redifferentiation in a proximal to distal sequence (most mature at proximal position: *osterix/osteocalcin/spp1* expression, followed by *runx2/osterix* expression, and *runx2* most distally).^(15,196) Lineage restriction of osteoblasts has been demonstrated during the regeneration process,^(15,166,167) much like for other cell types of the blastema.⁽¹⁹⁷⁾ Notably, mature stump osteoblasts are not the only source of osteoblasts in regeneration, and several other cell populations contribute to regenerated bone in zebrafish^(168,169) and medaka.⁽¹⁹⁸⁾ Thus, bone regeneration in teleost fin rays is highly plastic.⁽⁴¹⁾

Human bone traumata rarely include profound tissue removal, but often present as fractures or tissue necroses. In addition to a cryoinjury model, in which necrotic bone fragments get displaced from the wound margin,⁽¹⁹⁹⁾ bony fin ray fractures

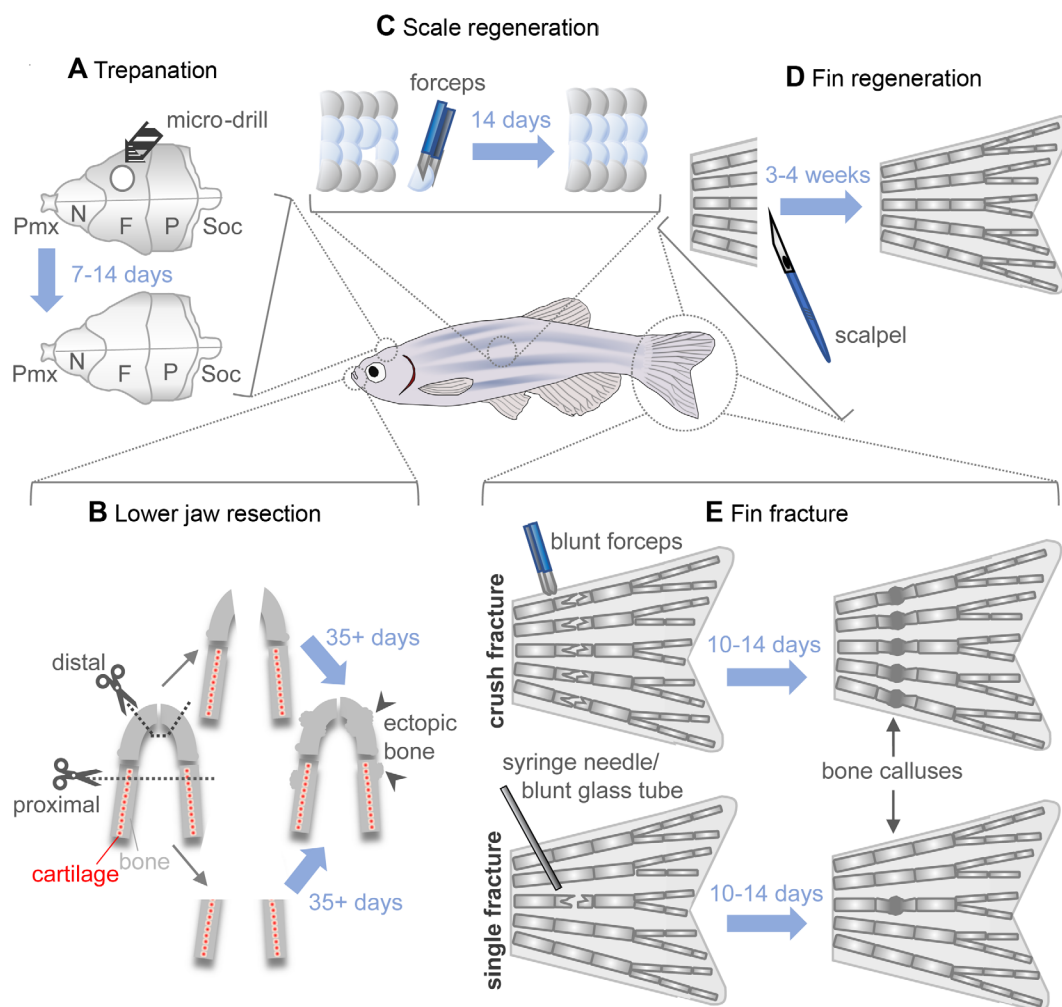


Fig 5. Models of bone repair and regeneration in adult zebrafish. (A) During skull trepanation, a microdrill is used to destroy bone from the os frontale, which regenerates within 7 to 14 days. (B) Two models of lower jaw resection can be performed: proximal, where both cartilage and bone are removed posterior to the synovial joint using surgical scissors (dotted line), and distal, where only the most anterior part of the bone is removed. Regeneration post resection takes upwards of 35 days and leads to ectopic bone formation in the regenerate. (C) Scale plucking with forceps is a simple method for studying bone regeneration *in vivo*. Scales can be cultured *ex vivo* and bone regeneration easily studied dynamically *in vivo* due to the superficial nature of the injury. (D) Due to its accessibility and the presence of lepidotrichia (bony fin rays), the caudal fin is an excellent model for studying bone regeneration and repair. Epimorphic fin regeneration after amputation requires 3 to 4 weeks until completion. (E) Fin ray fractures are bridged in 10 to 14 days and result in a bone callus, which is then remodeled. Two fin ray fracture models are available: in the crush-fracture model (top), forceps are used to introduce fractures along the entire width of the fin. In the single-fracture model, either a syringe needle or blunt glass capillary tube is used to press on an individual bone segment, introducing a single fracture in one or both hemirays. F = os frontale; N = os nasale; P = os parietale; Pmx = os premaxillare; Soc = os supraoccipitale.

are increasingly used to elucidate mechanisms of vertebrate bone repair (Table 1). To date, two main fin fracture models have been described: a crush injury model that affects several bony fin rays⁽¹³⁾ and a milder fracture model which only affects a single bony fin ray in usually one hemiray segment^(14,200) (Fig. 5E). Although there are differences between these two models, fracture repair in both involves a thickening of the tissue surrounding the lesion, reminiscent of the callus formed during mammalian fracture repair (Fig. 5E, Table 2). The molecular mechanisms and cellular dynamics underlying zebrafish fracture repair and fin regeneration are surprisingly similar. For example, dedifferentiation, migration and redifferentiation of osteoblasts

also occur during zebrafish fracture healing.^(13,14) Thus, it remains to be investigated which events truly distinguish fin fracture healing from fin regeneration after amputation. One important difference between mammalian and zebrafish fracture healing, however, concerns the contribution of osteoblast precursors from the BM. These BM-derived stromal cells take part in mammalian long-bone fracture repair,⁽²⁰¹⁾ but are absent in zebrafish, which lack BM proper. In contrast, osteoblast dedifferentiation has not been described in mammals⁽²⁰²⁾ with the exception of digit tip regeneration during which bone cells acquire a blastemal state to regenerate the tissue,^(16,17) and in bone explants.⁽²⁰³⁾ Future work needs to evaluate the relevance

Table 2. Overview on Zebrafish Bone Injury Paradigms and Mechanisms of Bone Restoration

Bone injury	Ossification	Callus formation	Osteoblast progenitor source		References
			De novo	Dedifferentiation-redifferentiation (in vivo)	
Zebrafish					
Skull	Intramembranous	No	?	Yes	(14)
Jaw	Intramembranous	Yes	Yes	? (yes)	(160–163)
Scale	Intramembranous	No	Yes	?	(23,164,165)
Fin amputation	Intramembranous	No	Yes	Yes	(15,166–169)
Fin fracture	Intramembranous	Yes	?	Yes	(13,14)
Mammals					
Tibia	Endochondral	Yes	Yes	?	(161,170)
Femur	Endochondral	Yes	Yes	?	(171)
Skull	Intramembranous	No	Yes	?	(170,172)

of osteoblast dedifferentiation for mammalian fracture repair and bone homeostasis.

In both mammals and in zebrafish, skull injuries (trepanations) are repaired by intramembranous ossification without callus formation (Table 2).⁽¹⁷⁰⁾ In zebrafish, trepanations have been performed by drilling a hole in the os frontale and/or os parietale^(14,200) (Fig. 5A). As with fin injury paradigms, trepanation of zebrafish calvariae induces mature osteoblasts to dedifferentiate,⁽¹⁴⁾ a mechanism that has not been tested for in mammalian skull injury models (Table 2). In contrast, calvarial bone healing in mammals might be mediated by stem cells at the sutures.⁽¹⁷²⁾

Zebrafish bones have some special gene expression features best exemplified by reference to jaw regeneration, which produces a hybrid cartilage-bone cell type. This cell type first produces cartilage and later switches to bone matrix mineralization.⁽¹⁶⁰⁾ Interestingly, hypertrophic chondrocytes give rise to osteoblasts in developing zebrafish ceratohyal bone,⁽²⁰⁴⁾ a phenomenon also observed in mammalian mandibular condyle⁽²⁰⁵⁾ and long-bone development.^(206,207) Besides this peculiarity, zebrafish jaw regeneration occurs by formation of a transient cartilage callus and involves a periosteal origin of bone-forming cells, similar to what has been reported in mammalian fracture repair.^(160–162) Surgical removal of jaw tissue in zebrafish, however, leads to wound epidermis and blastema formation,^(160,162,163) as well as activation of signaling cascades known from appendage regeneration in zebrafish and other nonmammalian vertebrates.^(208,209) Although jaw regeneration in zebrafish bridges wide skeletal gaps, it may result in a malformed shape with ectopic ossification of cartilage in the mandibular symphysis (Fig. 5B).^(162,163) Unlike other bone regeneration models in zebrafish, jaw regeneration involves callus formation and progenitor sources equivalent to bone healing in nonregenerative species. In humans, jaw regeneration is limited and methods for repairing the missing jaw tissue include distraction of the remaining mandibular bone or the use of implants, tissue transplants or, more recently, stem cells, although these therapies are not completely successful.⁽²¹⁰⁾ Hence, investigating differences between appendage and jaw regeneration in different species could lead to novel approaches for regenerative therapy in humans.

Another teleost bone structure with high regenerative capacity is the elasmoid scale, a dermal bone embedded in the skin (Fig. 5C). The scale is covered by osteoblasts on both sides and osteoclasts along mineral grooves (radii).⁽²¹¹⁾ As for appendages, the first stage of regeneration is wound reepithelialization.⁽¹⁶⁴⁾

Rapid reconstruction of the scale occurs by proliferation of a pool of de novo osteoblasts, shape changes, and cell death, resulting in three spatially distinct osteoblast populations.^(23,165) Osteoblasts then deposit collagen fibrils, and mineralization of the scale proceeds. Osteoclasts remodel the scale to its final shape.^(31,164,165,211)

Zebrafish have a high capacity to regenerate different skeletal tissues, and plasticity of bone forming cells may be the key to maintaining this ability. Understanding and identifying conserved regenerative mechanism in vertebrates that potentially have been lost in mammals will be important to modulate human bone regeneration in a clinical setting in the future.

Modeling Hormonal Bone Disorders in Zebrafish Fins and Scales

Metabolic and hormonal problems cause a wide range of human disorders that frequently involve bone.⁽²¹²⁾ Several related bone disease models, eg, mimicking osteoporosis-like phenotypes, have been developed in zebrafish,⁽²¹³⁾ often by using unique anatomical bone structures such as exoskeletal zebrafish fin rays or scales.⁽²¹⁴⁾

Zebrafish have been increasingly used to study the adverse effects of glucocorticoids (GCs), which cause GC-induced osteoporosis (GIO) in patients undergoing immunosuppressive treatment, on bone (Table 3). GC are mainly produced in the zebrafish interrenal gland within the head kidney,⁽²²⁸⁾ the equivalent of the adrenal cortex in mammals.⁽²²⁹⁾ Like humans,⁽²³⁰⁾ zebrafish have two GC receptor (GR) isoforms (gene *nr3c1*, nuclear receptor subfamily 3 group C member 1), GR α and GR β , which are nuclear hormone receptors, with a similar effective GR α /GR β ratio and predominantly nuclear localization.^(231,232) In contrast to humans, the zebrafish GR β does not function as a dominant negative inhibitor of the GR α isoform and is not transcriptionally active.^(233,234) Furthermore, zebrafish lack a direct homologue of *Hydroxysteroid 11-beta dehydrogenase 1* (11 β -HSD1)⁽²³⁵⁾ and therefore do not reduce 11-ketosteroid, which means that they are not able to activate GC from inactive precursors and thus exhibit a limited tissue-specific action.⁽²³⁶⁾ However, stress axis signaling is otherwise conserved in zebrafish.⁽²³⁷⁾ Importantly, zebrafish react to stress by producing the corticosteroid cortisol, like humans, whereas rodent species rely on corticosterone production upon stress.^(238,239) Moreover, active forms of GC can be used to circumvent the

Table 3. Overview on Bone Inhibitory Effects of Excess GC Levels in Zebrafish

Zebrafish model	Compound screen possible?	GC	Effect	Reference
Development	+	Dexamethasone	Inhibition of bone formation, downregulation of osteoblast-specific genes, reduced mineralized matrix in skull	(215–218)
		Prednisolone	Delayed and reduced mineralization, enriched NF- κ B and focal adhesion signaling pathway, increased osteoclast activity	(219–222)
Fin fold regeneration	+	Beclomethasone	Inhibited regeneration, less proliferating cells, inhibition of neutrophil migration	(223,224)
Scales	+	Beclomethasone dipropionate	Inhibited regeneration, mis-expression of <i>cripto-1</i>	(225)
		Dexamethasone	Decreased size and circularity in regenerating scales, suppressed osteoclast activity	(226)
		Prednisolone	Enhanced matrix breakdown, increased osteoclast activation	(159,227)
Adult fin regeneration	–	Prednisolone	Regenerates remain shorter, osteoblast proliferation and differentiation reduced, no increased osteoclast activity	(219)
		Beclomethasone	Transient activation of GR is sufficient to inhibit regeneration	(223)
Skull regeneration	–	Prednisolone	Complete, but slow regeneration	(219)

lack of 11 β -HSD1, which is why GC effects on bone can be well studied in zebrafish.⁽²³⁷⁾

In vivo manipulation of GR signaling is technologically advanced in zebrafish models, and a variety of zebrafish mutants and transgenic reporter lines have been generated to analyze GR signaling activity and GC resistance (Table 4). Several GR mutants exist today, such as the hypomorph *gr*^{s357(244)} and the null mutant *nr3c1*^{ia30/ia30}.⁽²⁴⁵⁾ Remarkably, zebrafish null mutant larvae have increased levels of whole-body cortisol, but nevertheless show relatively normal morphology and are viable through adulthood, in contrast to mice.⁽²⁴⁵⁾ A variety of transgenic zebrafish reporter lines, such as the Tg(6xGRE:EGFP,*myl7*:TagBFP) line, also known as SR4G,⁽²⁴⁰⁾ the Tg(GRE:Luciferase) line, which is used in a specially developed “glucocorticoid responsive in vivo zebrafish luciferase activity” (GRIZLY) assay,⁽²⁴²⁾ and the Tg(9xGCRE-*HSV.U123*:EGFP) line⁽²⁴¹⁾ are useful to monitor GR activity across zebrafish tissues in vivo. GC resistance can be visualized with the help of the Tg(*pomc*:GFP) line, in which the reaction to GC treatment can be monitored via the decrease of *pomc*

expression in the pituitary gland. A forward-genetic screen enabled the identification of GC-resistant zebrafish mutants, such as *loopless* (*lpl*), lacking *pomc* suppression.⁽²⁴³⁾ Notably, ubiquitous GR knockout in zebrafish leads to increased muscle mass,⁽²⁴⁷⁾ which could mechanically impact bone, too. Zebrafish can also be utilized to investigate the function of the mineralocorticoid receptor (MR) that is evolutionarily linked and cooperating with the GR.⁽²⁴⁸⁾ Recently, studies on the MR and GR showed that both receptors differentially regulate transcription, protein deposition, and proteolysis during larval development and that their combined activation is responsible for growth suppression.⁽²⁴⁹⁾

The mentioned tools can be used to model the effects of excess GC on bone. In embryos and larvae, models mimicking impaired bone formation as observed during GIO were established by using prednisolone^(219–221) and dexamethasone.^(215–217) Inhibited bone formation and mineralization linked to reduced expression of osteoblast-specific genes^(215–217,219,220) and increased osteoclast activity^(217,221)

Table 4. Tools to Study GR Signaling and GC Resistance in Zebrafish

Tool	Use/details	Reference
Reporter lines		
Tg(6xGRE:EGFP, <i>myl7</i> :TagBFP) ^{mn48}	Monitors GR activity, high-resolution model for physiological and stressed conditions	(240)
Tg(9xGCRE- <i>HSV.U123</i> :EGFP) ^{ia20}	Monitors GR activity, high responsiveness to GC treatment, endogenous stimuli, and molecular manipulation	(241)
Tg(GRE:Luciferase) ^{sb6}	Monitors GR activity, can be monitored in a specially developed GRIZLY assay	(242)
Tg(<i>pomc</i> :GFP) ^{zf44}	Monitors the reaction to GC treatment via <i>pomc</i> expression; visualization of GC resistance	(243)
Mutants		
<i>gr</i> ^{s357}	Hypomorph GR mutant	(244)
<i>nr3c1</i> ^{ia30/ia30} , <i>nr3c1</i> ^{ca402/ca402}	GR null mutants, hypercortisolemic, failing cortisol stress response	(245,246)
<i>loopless</i> <i>lpl</i> ^{hu6377}	GC resistant, lack <i>pomc</i> expression	(243)
<i>nr3c2</i> ^{ca402/ca402}	MR null mutant, delayed and dysregulated cortisol response	(246)

GRIZLY = glucocorticoid-responsive in vivo zebrafish luciferase activity.

were the most prominent effects observed. In 2-week-old, prednisolone-treated zebrafish, mRNA levels of *osterix* (*sp7*), osteocalcin (*bglap*), and *entpd5* were clearly reduced, whereas some matrix metalloproteases were induced.⁽²²²⁾ Excess GC levels have anti-regenerative effects in zebrafish. Larval fin fold regeneration was inhibited after prednisolone⁽²²³⁾ and beclomethasone dipropionate treatment, a process that was mediated by *cripto-1*, a Nodal signaling co-factor and Activin-signaling antagonist.⁽²²⁵⁾ Larval fin fold regeneration was not inhibited with the selective GR agonist ginsenoside Rg1.⁽²⁵⁰⁾ In adults, prednisolone treatment caused poor scale regeneration resulting from enhanced matrix breakdown due to increased osteoclast activity,^(159,227) and impaired fin regeneration,⁽²¹⁹⁾ also due to alterations in vesicular transport mechanisms.⁽²⁵¹⁾ Studies with beclomethasone suggest that a temporary activation of the GR during blastema formation is sufficient to block regeneration.⁽²²³⁾ Notably, antiosteoclastogenic effects were observed in fin regeneration and fin ray fracture healing following prednisolone treatment in zebrafish (Geurtzen and colleagues⁽²¹⁹⁾ and personal observations) and medaka.⁽²⁵²⁾ Vertebral bone volume and skull regeneration after trepanation were remarkably unaffected by prednisolone treatment.⁽²¹⁹⁾

Zebrafish are known for their use in drug screening approaches. High-throughput screens on larvae to identify anti-osteoporotic compounds have identified compounds such as RU486⁽²²⁰⁾ and tanshinol.⁽²¹⁵⁾ Another antiosteoporotic drug, the flavonoid icariin, which protects against Rankl-induced bone resorption, was identified in medaka embryos.⁽²⁵³⁾

Zebrafish scales are a useful tool for drug screening purposes and in vivo imaging.^(23,31) Scales are small and abundant, have transparent anatomical structures and can be cultured for up to 72 hours⁽³¹⁾ (Table 1). Transgenic reporter lines labeling osteoblasts are useful in this context.^(23,254) In terms of GC-related research, the scale model confirmed the bone protective function of the bisphosphonate alendronate⁽²²⁷⁾ and the vitamin D (vitD) homologue alfacalcidol.⁽²²⁶⁾ The scale model also holds promise to further elucidate close interactions of bone resident cells. Fractured zebrafish scales revealed a previously unrecognized cellular mechanism of osteoblast–osteoclast communication via osteoblast-derived extracellular vesicles promoting osteoclast differentiation.⁽²⁵⁵⁾

Low bone quality and increased fracture risk are a frequent consequence of diabetes mellitus.⁽²⁵⁶⁾ Both type I and type II diabetes mellitus have been modeled in zebrafish. Type I diabetic zebrafish, which were injected with the diabetogenic drug streptozocin, killing pancreatic beta-cells, showed impaired fin regeneration due to decreased proliferative potential in the regenerate.⁽²⁵⁷⁾ In type II diabetic zebrafish, which were incubated in high glucose, scales showed an imbalance in bone metabolism inducing an osteoporosis-like phenotype.⁽²⁵⁸⁾ Moreover, scale assays revealed that the antioxidant liquiritigenin counteracts osteoporotic complications in hyperglycemic fish.⁽²⁵⁹⁾ It will be interesting to investigate bone quality of other bones in diabetic zebrafish, such as the vertebrae and skull, and to characterize fracture repair in one of the available fracture models in the future.

As in mammals, vitD is suggested to play a role in increasing the available plasma phosphate in fish.⁽²⁶⁰⁾ Overexpression of *hand2*, which stimulates vitD inactivation, led to altered regeneration of bones in the zebrafish pectoral fin, which could be partially rescued by administration of vitD.⁽²⁶¹⁾ Likewise, vitD receptor inhibition suppressed fin regeneration, whereas vitD analogue treatment promoted fin regeneration.⁽²⁶²⁾ In vivo compound screening with larval zebrafish revealed dose-dependent increases in the formation of mineralized bone following vitD

and calcitriol administration.^(263,264) Furthermore, diabetic zebrafish treated with paricalcitol, a vitD analog, showed improved bone regeneration and mineralization due to enhanced osteoblast differentiation and insulin expression.⁽²⁶⁵⁾ These studies confirmed the importance of vitD for bone health in zebrafish. Altogether, the described work strengthened the importance of zebrafish for studying hormonal and metabolic bone disorders in nonmammalian species.

Larval Models to Study Bone Metastasis

Zebrafish are increasingly used to study bone disease related to secondary tumor formation. Bone metastases are common in cancer patients and associated with a poor prognosis. The composition of bone extracellular matrix with its embedded cells, growth factors, and chemokines makes it an attractive site for cancer cell homing.^(266–270) Crosstalk between bone and cancer cells leads to an imbalance between osteoblast-mediated bone formation and osteoclast-mediated bone resorption resulting in dysregulated bone remodeling (reviewed in Guise⁽²⁷¹⁾). Such interactions can promote bone metastasis formation.^(272,273)

Notably, although osteoblasts and osteoclasts have been shown to impact bone metastasis, many studies demonstrate that the mammalian BM is a particularly favorable environment for tumor cells (reviewed eg, in Schmid-Alliana and colleagues⁽²⁷⁴⁾). BM is not a mineralized tissue, but is of special interest to clinicians seeing cancer patients developing bone metastasis. In zebrafish larvae, bone formation and hematopoiesis take place in separate locations, which allows scientists to reveal the distinct roles of bone mineral and BM-like attractants for cancer cells. Mammalian BM expresses cancer cell attractants which is also true for the zebrafish caudal hematopoietic tissue (CHT) (Fig. 6). The cytoarchitecture and processes observed in the CHT resemble those of mammalian BM (Fig. 6A,B), which is why the CHT is often referred to as a BM-like niche. In zebrafish larvae, blood formation takes place in this vascular plexus in the ventral tail region of the growing zebrafish (Fig. 6A).⁽¹⁹⁾ Experimentally, it has been observed that some cancer cells home to the CHT leaving the circulation.^(275–277) This, together with the fact that cancer cells can be injected easily into zebrafish embryos and larvae, led to the establishment of zebrafish xenografts to study bone metastasis formation.

The CHT contains different cell types, including endothelial, lymphoid, myeloid, and mesenchymal stromal cells (MSCs) (Fig. 6A). Hematopoietic stem cells (HSCs) migrate to the zebrafish CHT niche in response to increased *chemokine* (*C-X-C*) *motif ligand 12a* (*cxcl12a*) expressed by MSCs.⁽²⁷⁸⁾ Although the CXCL12/CXCR4 (*C-X-C Motif Chemokine Receptor 4*) axis was already shown to exert an important role in cancer-endothelial cell adhesion,⁽²⁷⁹⁾ invasive activity modulation,⁽²⁸⁰⁾ and cancer cell proliferation⁽²⁸¹⁾ in mice, a growing number of zebrafish studies highlight the contribution of this signaling pathway to metastasis formation.^(282–284) The CHT also expresses *gata2b*, the orthologue of *Gata2*⁽²⁸⁵⁾ that regulates HSC maintenance within the BM⁽²⁸⁶⁾ and is associated with distant metastatic progression of prostate cancer.⁽²⁸⁷⁾

The CHT is highly vascularized and its endothelial cells can form a stem cell pocket to sustain HSCs.⁽²⁸⁸⁾ Endothelial cells in the CHT express *transcription factor EC* (*tfec*),⁽²⁸⁹⁾ *kit ligand b* (*kitlgb*),^(289,290) *oncostatin M* (*osm*),⁽²⁹⁰⁾ *kruppel-like factor 6a* (*klf6a*), *C-C motif chemokine ligand 25b* (*ccl25b*),⁽²⁹¹⁾ *chemokine* (*C-X-C motif*) *receptor 1* (*cxcr1*), and *chemokine* (*C-X-C motif*)

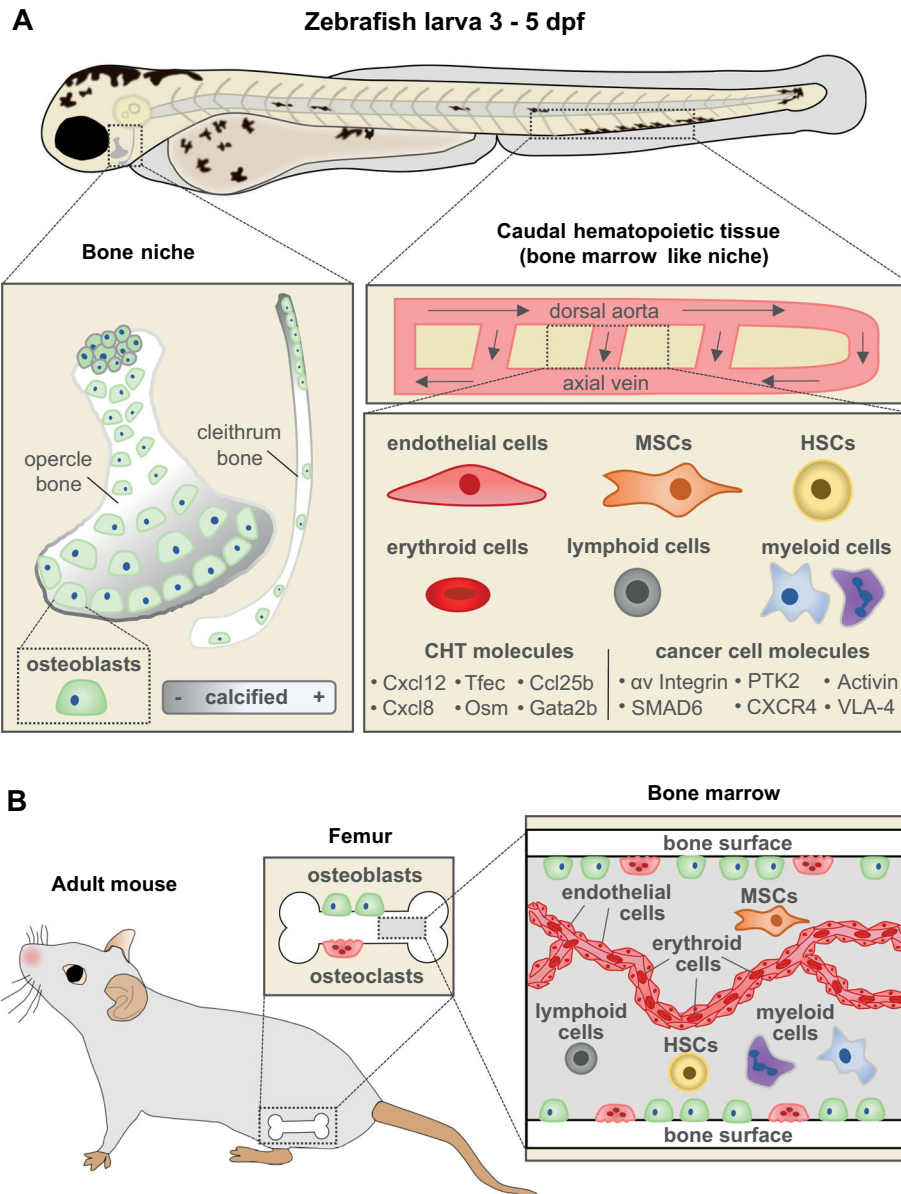


Fig 6. The CHT as an attractive site to study bone metastasis (A) Zebrafish larvae at 3 to 5 dpf contain developing bone (opercle and cleithrum) and CHT which acts as a BM-like niche. (Left) The opercle and cleithrum are among the first dermal bones to develop and can be imaged in live larvae due to their lateral, superficial positioning. (Right) The CHT is located laterally to the dorsal aorta in the posterior region of the larval zebrafish and is the site of early hematopoiesis, akin to mammalian BM. The cellular components of the CHT include endothelial cells, MSCs, HSCs, myeloid cells such as macrophages and neutrophils, lymphoid cells, and erythroid cells. Molecular components of the CHT listed have been previously shown to play a role in bone metastasis in mammalian models. Metastasis-related factors expressed in cancer cells uncovered in this model are shown on the right. (B) Illustration of the BM niche in a mouse long bone containing similar cell types as the CHT. dpf = days post fertilization; MSCs = mesenchymal stromal cells; HSCs = hematopoietic stem cells.

ligand 8a (cxcl8a)⁽²⁷⁸⁾ (Fig. 6A), which are responsible for HSC colonization and whose orthologues are partially expressed in BM and might contribute to metastasis formation.^(292–298)

Myeloid cells (neutrophils and macrophages), whose involvement in bone metastasis has been established in murine models,^(298,299) populate the CHT. In zebrafish, myeloid cell depletion results in breast cancer cell invasion in the proximity of the CHT.⁽²⁸⁴⁾

To induce metastasis in zebrafish, a variety of methods such as mutagenesis by carcinogens, targeted mutagenesis of tumor

suppressor genes, and tissue-specific overexpression of oncogenes are available.^(300–302) Xenografting, ie, the transfer of living cells between species, is a straightforward way to investigate the mechanisms underlying bone metastasis. The benefits of zebrafish larval xenografts include the possibility of high throughput, the ease of tracking of fluorescently labeled cancer cells due to optical clarity of larvae,⁽³⁰³⁾ and relatively fast micrometastasis development.^(304,305) Cancer cells can be injected into the blood stream via the duct of Cuvier (DoC), heart, and posterior cardinal vein of 2 dpf larvae in which adaptive immunity is absent.^(276,306)

Homing of cancer cells to new sites requires extravasation and resembles micrometastasis formation, which can be observed within a few days post injection at sites such as the CHT, fin fold, and trunk.^(284,305,307)

The larval xenograft model has been employed to investigate bone metastasis of prostate cancer, breast cancer, and multiple myeloma (MM) in the CHT and studied regarding the molecules and signaling pathways involved^(276,308–312) (Fig. 6A). Human prostate cancer cells, resected from the CHT several days post-DoC injection, were found to upregulate stemness (eg, *NANOG*, *OCT4*, *Cripto*, *C-X-C Motif Chemokine Ligand 2* [*CXCL2*]) and mesenchymal (eg, *Vimentin*, *Twist*, and *Zinc Finger E-Box Binding Homeobox 2* [*ZEB2*]) markers while reducing E-cadherin.⁽³⁰⁸⁾ Moreover, the CHT microenvironment enhanced Activin A expression, which correlates with increased bone metastasis risk in patients, in prostate cancer cells.⁽³⁰⁹⁾

The zebrafish xenograft model has been used to study micrometastasis formation of triple-negative breast cancer (TNBC). High *CXCR4* expressing TNBC cells progressively extravasated and invaded the CHT, more than cells displaying low *CXCR4* mRNA levels.⁽²⁸³⁾ Importantly, *CXCR4* sustained tumor metastasis in a *Cxcl12*-dependent manner, which resembles the situation in human and murine models of breast cancer.

Several other signaling pathways were found to drive breast cancer metastases in the zebrafish CHT (Fig. 6A). Similar experiments demonstrated the importance of *SMAD6*⁽³¹⁰⁾ and α v integrin⁽³¹¹⁾ for invasion of TNBC. Depletion of α v integrin caused a decrease of *SNAIL*, *SLUG*, *N-Cadherin*, and *Vimentin* expression, and resulted in a dramatic decrease of invasion and metastases.

At the time patients are diagnosed with MM, various BM-lytic lesions can often be observed.⁽³¹²⁾ In zebrafish, MM cell homing to the CHT increased gene expression in cancer cells related to cytokine and chemokine-mediated signaling (including IL-6), cell adhesion, and angiogenesis,⁽²⁷⁶⁾ signals known from the mammalian BM microenvironment.^(313–315) Reduced expression of Very Late Antigen 4 (VLA-4), PTK2 protein tyrosine kinase 2 (PTK2 or FAK), and *CXCR4* led to impaired homing of MM cells to the CHT,⁽²⁷⁶⁾ demonstrating the similarity of CHT metastasis to processes observed in mammalian BM.^(316–318)

An advantage of zebrafish xenografts is the possibility to test drug regimes on human tumor material in a semi-high-throughput manner. Tumor cells can also be pretreated with chemical compounds and injected into zebrafish to observe their effect on tumor growth and progression.⁽²⁸³⁾ Examples of drugs tested in zebrafish xenotransplants include R-406 inhibiting SYK kinase for retinoblastoma⁽³¹⁹⁾ and prostate cancer metastasis,⁽³²⁰⁾ gomesin and gomesin-like homologue for melanoma,⁽³²¹⁾ and IT1t, a *CXCR4* antagonists, for breast cancer metastasis.⁽²⁸³⁾ These and other examples demonstrate the power of zebrafish screens to identify promising drugs as potential cancer metastases treatments. Together with the high-resolution in vivo imaging this will further promote zebrafish as a preclinical animal model in cancer research.

Conclusions

Zebrafish are increasingly used in the field of skeletal disease and regeneration research because of their ease of genetic manipulation, convenient drug treatment options, and in vivo imaging possibilities. High-throughput genetic and drug screening can be performed in zebrafish larvae, which can also be used as xenograft recipients to study bone metastasis. There are many

similarities between mammalian and zebrafish physiology, which allow the investigation of hormonal bone disease in zebrafish. Zebrafish bones regenerate remarkably well, and high plasticity of bone-forming cells might be key to this ability. Understanding the pathogenesis of skeletal alterations and regeneration in zebrafish will help to improve therapeutic approaches in a clinical setting in the future.

Disclosures

All authors declare no competing financial interest.

Acknowledgments

This work was supported by the Deutsche Forschungsgemeinschaft (DFG) Transregio 67 (project 387653785 to FK) and the DFG SPP 2084 μ Bone (projects B2562/6-1 and KN 1102/2-1, to BB and FK, respectively). AK has been a Deutscher Akademischer Austauschdienst (DAAD) fellow during this work. The work of FK is co-financed with tax revenues based on the budget agreed by the Saxonian Landtag. Further funding of IAKF and BB was received from the Interdisciplinary Center for Interface Research (ICCIR) and the Forum Medical Technology Health Hamburg (FMTHH) on behalf of the Hamburg University of Technology (TUHH) and the University Medical Center Hamburg-Eppendorf (UKE). CLH was supported by Versus Arthritis Senior Fellowship 21937, and LMM by the Wellcome Trust Dynamic Molecular Cell Biology doctoral training program. Our thanks go to Henriette Knopf for proofreading the manuscript and to Heiner Grandel for valuable comments. Open Access funding enabled and organized by ProjektDEAL.

Authors' roles: all authors wrote and revised the manuscript.

AUTHOR CONTRIBUTIONS

Kristin Dietrich: Writing-original draft; writing-review & editing. **Imke Fiedler:** Visualization; writing-original draft; writing-review & editing. **Anastasia Kurzyukova:** Visualization; writing-original draft; writing-review & editing. **Alejandra Lopez Delgado:** Visualization; writing-original draft; writing-review & editing. **Lucy McGowan:** Visualization; writing-original draft; writing-review & editing. **Karina Geurtzen:** Writing-original draft; writing-review & editing. **Chrissy Hammond:** Writing-original draft; writing-review & editing. **Björn Busse:** Writing-original draft; writing-review & editing. **Franziska Knopf:** Conceptualization; writing-original draft; writing-review & editing.

References

1. Spoorendonk KM, Hammond CL, Huitema LFA, Vanoevelen J, Schulte-Merker S. Zebrafish as a unique model system in bone research: the power of genetics and in vivo imaging. *J Appl Ichthyol*. 2010;26(2):219-224.
2. Busse B, Galloway JL, Gray RS, Harris MP, Kwon RY. Zebrafish: an emerging model for orthopedic research. *J Orthop Res*. 2020;38(5):925-936.
3. Xu C, Volkery S, Siekmann AF. Intubation-based anesthesia for long-term time-lapse imaging of adult zebrafish. *Nat Protoc*. 2015;10(12):2064-2073.
4. Hammond CL, Moro E. Using transgenic reporters to visualize bone and cartilage signaling during development in vivo. *Front Endocrinol (Lausanne)*. 2012;3:91.

5. Weigelt J, Franz-Odenaal TA. Functional bone histology of zebrafish reveals two types of endochondral ossification, different types of osteoblast clusters and a new bone type. *J Anat.* 2016;229(1): 92-103.
6. Witten PE, Hansen A, Hall BK. Features of mono- and multinucleated bone resorbing cells of the zebrafish *Danio rerio* and their contribution to skeletal development, remodeling, and growth. *J Morphol.* 2001;250(3):197-207.
7. Tonelli F, Bek JW, Besio R, et al. Zebrafish: a resourceful vertebrate model to investigate skeletal disorders. *Front Endocrinol.* 2020; 11:489.
8. Spence R, Smith C. Mating preference of female zebrafish, *Danio rerio*, in relation to male dominance. *Behav Ecol.* 2006;17(5): 779-783.
9. Li N, Felber K, Elks P, Croucher P, Roehl HH. Tracking gene expression during zebrafish osteoblast differentiation. *Dev Dyn.* 2009; 238(2):459-466.
10. Ogata S, Uthoff HK. The early development and ossification of the human clavicle—an embryologic study. *Acta Orthop Scand.* 1990; 61(4):330-334.
11. Bergen DJM, Kague E, Hammond CL. Zebrafish as an emerging model for osteoporosis: a primary testing platform for screening new osteo-active compounds. *Front Endocrinol (Lausanne).* 2019; 10:6.
12. Newham E, Kague E, Aggleton JA, Ferner C, Brown KR, Hammond CL. Finite element and deformation analyses predict pattern of bone failure in loaded zebrafish spines. *J R Soc Interface.* 2019;16(160):20190430.
13. Sousa S, Valerio F, Jacinto A. A new zebrafish bone crush injury model. *Biol Open.* 2012;1(9):915-921.
14. Geurtzen K, Knopf F, Wehner D, Huitema LF, Schulte-Merker S, Weidinger G. Mature osteoblasts dedifferentiate in response to traumatic bone injury in the zebrafish fin and skull. *Development.* 2014;141(11):2225-2234.
15. Knopf F, Hammond C, Chekuru A, et al. Bone regenerates via dedifferentiation of osteoblasts in the zebrafish fin. *Dev Cell.* 2011;20(5): 713-724.
16. Serowoky MA, Arata CE, Crump JG, Mariani FV. Skeletal stem cells: insights into maintaining and regenerating the skeleton. *Development.* 2020;147(5):dev179325.
17. Storer MA, Mahmud N, Karamboulas K, et al. Acquisition of a unique mesenchymal precursor-like blastema state underlies successful adult mammalian digit tip regeneration. *Dev Cell.* 2020;52(4):509-524.e9.
18. Howe K, Clark MD, Torroja CF, et al. The zebrafish reference genome sequence and its relationship to the human genome. *Nature.* 2013; 496(7446):498-503.
19. Murayama E, Kissa K, Zapata A, et al. Tracing hematopoietic precursor migration to successive hematopoietic organs during zebrafish development. *Immunity.* 2006;25(6):963-975.
20. Bensimon-Brito A, Carreira J, Dionisio G, Hysseune A, Cancela ML, Witten PE. Revisiting in vivo staining with alizarin red S: a valuable approach to analyse zebrafish skeletal mineralization during development and regeneration. *BMC Dev Biol.* 2016;16:2.
21. Frost HM. Tetracycline-based histological analysis of bone remodeling. *Calcif Tissue Res.* 1969;3(1):211-237.
22. Dempster DW, Compston JE, Drezner MK, et al. Standardized nomenclature, symbols, and units for bone histomorphometry: a 2012 update of the report of the ASBMR Histomorphometry Nomenclature Committee. *J Bone Miner Res.* 2013;28(1):2-17.
23. Cox BD, De Simone A, Tornini VA, Singh SP, Di Talia S, Poss KD. In toto imaging of dynamic osteoblast behaviors in regenerating skeletal bone. *Curr Biol.* 2018;28(24):3937-47.e4.
24. White RM, Sessa A, Burke C, et al. Transparent adult zebrafish as a tool for in vivo transplantation analysis. *Cell Stem Cell.* 2008;2(2): 183-189.
25. Hur M, Gistelinck CA, Huber P, et al. MicroCT-based phenomics in the zebrafish skeleton reveals virtues of deep phenotyping in a distributed organ system. *Elife.* 2017;6:e26014.
26. Whittier DE, Boyd SK, Burghardt AJ, et al. Guidelines for the assessment of bone density and microarchitecture in vivo using high-resolution peripheral quantitative computed tomography. *Osteoporos Int.* 2020;31(9):1607-1627.
27. Boutroy S, Bouxsein ML, Munoz F, Delmas PD. In vivo assessment of trabecular bone microarchitecture by high-resolution peripheral quantitative computed tomography. *J Clin Endocrinol Metab.* 2005;90(12):6508-6515.
28. Shah AN, Davey CF, Whitebitch AC, Miller AC, Moens CB. Rapid reverse genetic screening using CRISPR in zebrafish. *Nat Methods.* 2015;12(6):535-540.
29. Watson CJ, Monstad-Rios AT, Bhimani RM, et al. Phenomics-based quantification of CRISPR-induced mosaicism in zebrafish. *Cell Syst.* 2020;10(3):275-86.e5.
30. Ablain J, Durand EM, Yang S, Zhou Y, Zon LI. A CRISPR/Cas9 vector system for tissue-specific gene disruption in zebrafish. *Dev Cell.* 2015;32(6):756-764.
31. Pasqualetti S, Banfi G, Mariotti M. The zebrafish scale as model to study the bone mineralization process. *J Mol Histol.* 2012;43(5): 589-595.
32. Chekuru A, Kuscha V, Hans S, Brand M. Ligand-controlled site-specific recombination in zebrafish. *Methods Mol Biol.* 2017;1642: 87-97.
33. Nasevicius A, Ekker SC. Effective targeted gene 'knockdown' in zebrafish. *Nat Genet.* 2000;26(2):216-220.
34. Gibert Y, Trengrove MC, Ward AC. Zebrafish as a genetic model in pre-clinical drug testing and screening. *Curr Med Chem.* 2013;20 (19):2458-2466.
35. Wienholds E, van Eeden F, Kusters M, Mudde J, Plasterk RH, Cuppen E. Efficient target-selected mutagenesis in zebrafish. *Genome Res.* 2003;13(12):2700-2707.
36. Tessadori F, Roessler HI, Savelberg SMC, et al. Effective CRISPR/Cas9-based nucleotide editing in zebrafish to model human genetic cardiovascular disorders. *Dis Model Mech.* 2018;11(10): dmm035469.
37. Prykhodzhiy SV, Fuller C, Steele SL, et al. Optimized knock-in of point mutations in zebrafish using CRISPR/Cas9. *Nucleic Acids Res.* 2018; 46(17):e102.
38. Nguyen AT, Emelyanov A, Koh CH, Spitsbergen JM, Parinov S, Gong Z. An inducible kras(V12) transgenic zebrafish model for liver tumorigenesis and chemical drug screening. *Dis Model Mech.* 2012; 5(1):63-72.
39. Lleras-Forero L, Winkler C, Schulte-Merker S. Zebrafish and medaka as models for biomedical research of bone diseases. *Dev Biol.* 2020; 457(2):191-205.
40. Kwon RY, Watson CJ, Karasik D. Using zebrafish to study skeletal genomics. *Bone.* 2019;126:37-50.
41. Sehring IM, Weidinger G. Recent advancements in understanding fin regeneration in zebrafish. *Wiley Interdiscip Rev Dev Biol.* 2020; 9(1):e367.
42. Luderman LN, Unlu G, Knapik EW. Zebrafish developmental models of skeletal diseases. *Curr Top Dev Biol.* 2017;124:81-124.
43. Hirasawa T, Kuratani S. Evolution of the vertebrate skeleton: morphology, embryology, and development. *Zoological Lett.* 2015;1 (1):2.
44. Cubbage CC, Mabee PM. Development of the cranium and paired fins in the zebrafish *Danio rerio* (Ostariophysi, Cyprinidae). *J Morphol.* 1996;229(2):121-160.
45. Fisher S, Jagadeeswaran P, Halpern ME. Radiographic analysis of zebrafish skeletal defects. *Dev Biol.* 2003;264(1):64-76.
46. Gerhard GS. Comparative aspects of zebrafish (*Danio rerio*) as a model for aging research. *Exp Gerontol.* 2003;38(11-12):1333-1341.
47. Eames BF, DeLaurier A, Ullmann B, et al. FishFace: interactive atlas of zebrafish craniofacial development at cellular resolution. *BMC Dev Biol.* 2013;13:23.
48. Mork L, Crump G. Zebrafish craniofacial development: a window into early patterning. *Curr Top Dev Biol.* 2015;115:235-269.

49. Quarto N, Longaker MT. The zebrafish (*Danio rerio*): a model system for cranial suture patterning. *Cells Tissues Organs*. 2005;181(2):109-118.
50. Smeeton J, Askary A, Crump JG. Building and maintaining joints by exquisite local control of cell fate. *Wiley Interdiscip Rev Dev Biol*. 2017;6(1):e245.
51. Boswell CW, Ciruna B. Understanding idiopathic scoliosis: a new zebrafish school of thought. *Trends Genet*. 2017;33(3):183-196.
52. Bird NC, Mabee PM. Developmental morphology of the axial skeleton of the zebrafish, *Danio rerio* (Ostariophysi: Cyprinidae). *Dev Dyn*. 2003;228(3):337-357.
53. Bagnat M, Gray RS. Development of a straight vertebrate body axis. *Development*. 2020;147(21):dev175794.
54. Minchin JEN, Rawls JF. A classification system for zebrafish adipose tissues. *Dis Model Mech*. 2017;10(6):797.
55. Khajuria DK, Karasik D. Novel model of restricted mobility induced osteopenia in zebrafish. *J Fish Biol*. 2020;1-8. <https://doi.org/10.1111/jfb.14369>.
56. Suniaga S, Rolvien T, Vom Scheidt A, et al. Increased mechanical loading through controlled swimming exercise induces bone formation and mineralization in adult zebrafish. *Sci Rep*. 2018;8(1):3646.
57. Monma Y, Shimada Y, Nakayama H, Zang L, Nishimura N, Tanaka T. Aging-associated microstructural deterioration of vertebra in zebrafish. *Bone Rep*. 2019;11:100215.
58. Fiedler IAK, Schmidt FN, Wolfel EM, et al. Severely impaired bone material quality in Chihuahua zebrafish resembles classical dominant human osteogenesis imperfecta. *J Bone Miner Res*. 2018;33(8):1489-1499.
59. Ding Y, Vanselow DJ, Yakovlev MA, et al. Computational 3D histological phenotyping of whole zebrafish by X-ray histotomography. *Elife*. 2019;8:e44898.
60. Hayes AJ, Reynolds S, Nowell MA, et al. Spinal deformity in aged zebrafish is accompanied by degenerative changes to their vertebrae that resemble osteoarthritis. *PLoS One*. 2013;8(9):e75787.
61. Sakata-Haga H, Uchishiba M, Shimada H, et al. A rapid and nondestructive protocol for whole-mount bone staining of small fish and *Xenopus*. *Sci Rep*. 2018;8(1):7453.
62. Vagberg W, Larsson DH, Li M, Arner A, Hertz HM. X-ray phase-contrast tomography for high-spatial-resolution zebrafish muscle imaging. *Sci Rep*. 2015;5:16625.
63. Gaunt SJ, Sharpe PT, Duboule D. Spatially restricted domains of homeo-gene transcripts in mouse embryos: relation to a segmented body plan. *Development*. 1988;104(Suppl):169.
64. Burke AC, Nelson CE, Morgan BA, Tabin C. Hox genes and the evolution of vertebrate axial morphology. *Development*. 1995;121(2):333-346.
65. Bondos SE, Geraldo Mendes G, Jons A. Context-dependent HOX transcription factor function in health and disease. In Uversky VN, ed. *Progress in molecular biology and translational science*. Cambridge, MA: Academic Press; 2020 pp 225-262.
66. Quinonez SC, Innis JW. Human HOX gene disorders. *Mol Genet Metab*. 2014;111(1):4-15.
67. Prince VE, Joly L, Ekker M, Ho RK. Zebrafish hox genes: genomic organization and modified colinear expression patterns in the trunk. *Development*. 1998;125(3):407-420.
68. Amores A, Force A, Yan YL, et al. Zebrafish hox clusters and vertebrate genome evolution. *Science*. 1998;282(5394):1711-1714.
69. Duboule D. The rise and fall of Hox gene clusters. *Development*. 2007;134(14):2549-2560.
70. Morin-Kensicki EM, Melancon E, Eisen JS. Segmental relationship between somites and vertebral column in zebrafish. *Development*. 2002;129(16):3851-3860.
71. Freitas R, Zhang G, Cohn MJ. Evidence that mechanisms of fin development evolved in the midline of early vertebrates. *Nature*. 2006;442(7106):1033-1037.
72. Sordino P, van der Hoeven F, Duboule D. Hox gene expression in teleost fins and the origin of vertebrate digits. *Nature*. 1995;375(6533):678-681.
73. Ahn D, Ho RK. Tri-phasic expression of posterior Hox genes during development of pectoral fins in zebrafish: implications for the evolution of vertebrate paired appendages. *Dev Biol*. 2008;322(1):220-233.
74. Sheth R, Bastida MF, Kmita M, Ros M. "Self-regulation," a new facet of Hox genes' function. *Dev Dyn*. 2014;243(1):182-191.
75. Grandel H, Draper BW, Schulte-Merker S. Dackel acts in the ectoderm of the zebrafish pectoral fin bud to maintain AER signaling. *Development*. 2000;127(19):4169-4178.
76. Ng JK, Kawakami Y, Buscher D, et al. The limb identity gene *Tbx5* promotes limb initiation by interacting with *Wnt2b* and *Fgf10*. *Development*. 2002;129(22):5161-5170.
77. Gibert Y, Gajewski A, Meyer A, Begemann G. Induction and prepattern of the zebrafish pectoral fin bud requires axial retinoic acid signaling. *Development*. 2006;133(14):2649-2659.
78. Mercader N, Fischer S, Neumann CJ. *Prdm1* acts downstream of a sequential RA, Wnt and Fgf signaling cascade during zebrafish forelimb induction. *Development*. 2006;133(15):2805-2815.
79. Grandel H, Brand M. Zebrafish limb development is triggered by a retinoic acid signal during gastrulation. *Dev Dyn*. 2011;240(5):1116-1126.
80. Mercader N. Early steps of paired fin development in zebrafish compared with tetrapod limb development. *Dev Growth Differ*. 2007;49(6):421-437.
81. Loomis CA, Harris E, Michaud J, Wurst W, Hanks M, Joyner AL. The mouse *Engrailed-1* gene and ventral limb patterning. *Nature*. 1996;382(6589):360-363.
82. Sheth R, Marcon L, Bastida MF, et al. Hox genes regulate digit patterning by controlling the wavelength of a Turing-type mechanism. *Science*. 2012;338(6113):1476-1480.
83. Apschner A, Schulte-Merker S, Witten PE. Not all bones are created equal—using zebrafish and other teleost species in osteogenesis research. *Methods Cell Biol*. 2011;105:239-255.
84. Wopat S, Bagwell J, Sumigray KD, et al. Spine patterning is guided by segmentation of the notochord sheath. *Cell Rep*. 2018;22(8):2026-2038.
85. Inohaya K, Takano Y, Kudo A. The teleost intervertebral region acts as a growth center of the centrum: in vivo visualization of osteoblasts and their progenitors in transgenic fish. *Dev Dyn*. 2007;236(11):3031-3046.
86. Edsall SC, Franz-Odenaal TA. A quick whole-mount staining protocol for bone deposition and resorption. *Zebrafish*. 2010;7(3):275-280.
87. Witten PE, Harris MP, Huysseune A, Winkler C. Small teleost fish provide new insights into human skeletal diseases. *Methods Cell Biol*. 2017;138:321-346.
88. Mahamid J, Sharir A, Addadi L, Weiner S. Amorphous calcium phosphate is a major component of the forming fin bones of zebrafish: indications for an amorphous precursor phase. *Proc Natl Acad Sci U S A*. 2008;105(35):12748-12753.
89. Akiva A, Malkinson G, Masic A, et al. On the pathway of mineral deposition in larval zebrafish caudal fin bone. *Bone*. 2015;75:192-200.
90. Bennet M, Akiva A, Faivre D, et al. Simultaneous Raman microspectroscopy and fluorescence imaging of bone mineralization in living zebrafish larvae. *Biophys J*. 2014;106(4):L17-L19.
91. Wang X-M, Cui F-Z, Ge J, Ma C. Alterations in mineral properties of zebrafish skeletal bone induced by *liliputdtc232* gene mutation. *J Cryst Growth*. 2003;258(3):394-401.
92. Bijvelds MJ, Velden JA, Kolar ZI, Flik G. Magnesium transport in freshwater teleosts. *J Exp Biol*. 1998;201(Pt 13):1981-1990.
93. Siccardi AJ 3rd, Padgett-Vasquez S, Garriss HW, Nagy TR, D'Abramo LR, Watts SA. Dietary strontium increases bone mineral density in intact zebrafish (*Danio rerio*): a potential model system for bone research. *Zebrafish*. 2010;7(3):267-273.
94. Chang Z, Chen PY, Chuang YJ, Akhtar R. Zebrafish as a model to study bone maturation: nanoscale structural and mechanical characterization of age-related changes in the zebrafish vertebral column. *J Mech Behav Biomed Mater*. 2018;84:54-63.

95. Costa JM, Sartori MMP, Nascimento NFD, et al. Inadequate dietary phosphorus levels cause skeletal anomalies and alter osteocalcin gene expression in zebrafish. *Int J Mol Sci.* 2018;19(2):364.
96. Cotti S, Huyseune A, Koppe W, et al. More bone with less minerals? The effects of dietary phosphorus on the post-cranial skeleton in zebrafish. *Int J Mol Sci.* 2020;21(15):5429.
97. Roschger P, Fratzi P, Eschberger J, Klaushofer K. Validation of quantitative backscattered electron imaging for the measurement of mineral density distribution in human bone biopsies. *Bone.* 1998; 23(4):319-326.
98. Zimmermann EA, Busse B, Ritchie RO. The fracture mechanics of human bone: influence of disease and treatment. *Bonekey Rep.* 2015;4:743.
99. Zimmermann EA, Schaible E, Bale H, et al. Age-related changes in the plasticity and toughness of human cortical bone at multiple length scales. *Proc Natl Acad Sci U S A.* 2011;108(35):14416-14421.
100. Zhang Y, Cui FZ, Wang XM, Feng QL, Zhu XD. Mechanical properties of skeletal bone in gene-mutated *dtl28d* and wild-type zebrafish (*Danio rerio*) measured by atomic force microscopy-based nanoindentation. *Bone.* 2002;30(4):541-546.
101. Thurner PJ. Atomic force microscopy and indentation force measurement of bone. *Wiley Interdiscip Rev Nanomed Nanobiotechnol.* 2009;1(6):624-649.
102. Goretti Penido M, Alon US. Phosphate homeostasis and its role in bone health. *Pediatr Nephrol.* 2012;27(11):2039-2048.
103. Huitema LF, Apschner A, Logister I, et al. *Entpd5* is essential for skeletal mineralization and regulates phosphate homeostasis in zebrafish. *Proc Natl Acad Sci U S A.* 2012;109(52):21372-21377.
104. Apschner A, Huitema LF, Ponsioen B, Peterson-Maduro J, Schulte-Merker S. Zebrafish *enpp1* mutants exhibit pathological mineralization, mimicking features of generalized arterial calcification of infancy (GACI) and pseudoxanthoma elasticum (PXE). *Dis Model Mech.* 2014;7(7):811-822.
105. Verbruggen SW, Oyen ML, Phillips AT, Nowlan NC. Function and failure of the fetal membrane: modelling the mechanics of the chorion and amnion. *PLoS One.* 2017;12(3):e0171588.
106. Felsenthal N, Zelzer E. Mechanical regulation of musculoskeletal system development. *Development.* 2017;144(23):4271-4283.
107. Nowlan NC. Biomechanics of foetal movement. *Eur Cell Mater.* 2015; 29:1-21 discussion 21.
108. Pitsillides AA. Early effects of embryonic movement: 'a shot out of the dark'. *J Anat.* 2006;208(4):417-431.
109. Shwartz Y, Farkas Z, Stern T, Aszodi A, Zelzer E. Muscle contraction controls skeletal morphogenesis through regulation of chondrocyte convergent extension. *Dev Biol.* 2012;370(1):154-163.
110. Brunt LH, Skinner RE, Roddy KA, Araujo NM, Rayfield EJ, Hammond CL. Differential effects of altered patterns of movement and strain on joint cell behaviour and skeletal morphogenesis. *Osteoarthr Cartil.* 2016;24(11):1940-1950.
111. Brunt LH, Begg K, Kague E, Cross S, Hammond CL. Wnt signalling controls the response to mechanical loading during zebrafish joint development. *Development.* 2017;144(15):2798-2809.
112. Brunt LH, Roddy KA, Rayfield EJ, Hammond CL. Building finite element models to investigate zebrafish jaw biomechanics. *J Vis Exp.* 2016;118:54811.
113. Lawrence EA, Kague E, Aggleton JA, Harniman RL, Roddy KA, Hammond CL. The mechanical impact of *col11a2* loss on joints; *col11a2* mutant zebrafish show changes to joint development and function, which leads to early-onset osteoarthritis. *Philos Trans R Soc Lond B Biol Sci.* 2018;373(1759):20170335.
114. Askary A, Smeeton J, Paul S, et al. Ancient origin of lubricated joints in bony vertebrates. *Elife.* 2016;5:e16415.
115. Baird DA, Paternoster L, Gregory JS, et al. Investigation of the relationship between susceptibility loci for hip osteoarthritis and dual X-ray absorptiometry-derived hip shape in a population-based cohort of perimenopausal women. *Arthritis Rheumatol.* 2018;70(12):1984-1993.
116. Wilkinson JM, Zeggini E. The genetic epidemiology of joint shape and the development of osteoarthritis. *Calcif Tissue Int.* 2020. <https://doi.org/10.1007/s00223-020-00702-6>
117. Spoorendonk KM, Peterson-Maduro J, Renn J, et al. Retinoic acid and *Cyp26b1* are critical regulators of osteogenesis in the axial skeleton. *Development.* 2008;135(22):3765-3774.
118. Fiaz AW, Leon-Kloosterziel KM, Gort G, Schulte-Merker S, van Leeuwen JL, Kranenburg S. Swim-training changes the spatio-temporal dynamics of skeletogenesis in zebrafish larvae (*Danio rerio*). *PLoS One.* 2012;7(4):e34072.
119. Delgado-Calle J, Sato AY, Bellido T. Role and mechanism of action of sclerostin in bone. *Bone.* 2017;96:29-37.
120. Atkins A, Milgram J, Weiner S, Shahar R. The response of anosteocytic bone to controlled loading. *J Exp Biol.* 2015;218(Pt 22):3559-3569.
121. Ofer L, Dean MN, Zaslansky P, et al. A novel nonosteocytic regulatory mechanism of bone modeling. *PLoS Biol.* 2019;17(2):e3000140.
122. Grimm D, Grosse J, Wehland M, et al. The impact of microgravity on bone in humans. *Bone.* 2016;87:44-56.
123. Chatani M, Morimoto H, Takeyama K, et al. Acute transcriptional up-regulation specific to osteoblasts/osteoclasts in medaka fish immediately after exposure to microgravity. *Sci Rep.* 2016;6:39545.
124. Chatani M, Mantoku A, Takeyama K, et al. Microgravity promotes osteoclast activity in medaka fish reared at the international space station. *Sci Rep.* 2015;5:14172.
125. Lawrence EA, Aggleton JA, Loon JJWAv, et al. Exposure to hypergravity during zebrafish development alters cartilage material properties and strain distribution. *Bone & Joint Research.* 2020;10:2. <https://doi.org/10.1101/2020.05.26.116046>.
126. Aceto J, Nourizadeh-Lillabadi R, Maree R, et al. Zebrafish bone and general physiology are differentially affected by hormones or changes in gravity. *PLoS One.* 2015;10(6):e0126928.
127. Marini JC, Forlino A, Bachinger HP, et al. Osteogenesis imperfecta. *Nat Rev Dis Primers.* 2017;3:17052.
128. Nijhuis WH, Eastwood DM, Allgrove J, et al. Current concepts in osteogenesis imperfecta: bone structure, biomechanics and medical management. *J Child Orthop.* 2019;13(1):1-11.
129. Gistelincx K, Kwon RY, Malfait F, et al. Zebrafish type I collagen mutants faithfully recapitulate human type I collagenopathies. *Proc Natl Acad Sci U S A.* 2018;115(34):E8037-E8046.
130. Gioia R, Tonelli F, Ceppi I, et al. The chaperone activity of 4PBA ameliorates the skeletal phenotype of Chihuahua, a zebrafish model for dominant osteogenesis imperfecta. *Hum Mol Genet.* 2017;26(15): 2897-2911.
131. Caparrós-Martín JA, Martínez-Glez V, Valencia M, et al. BMP1 mutations in autosomal recessive osteogenesis imperfecta. In Shapiro JR, Byers PH, Glorieux FH, Sponseller P, eds. *Osteogenesis imperfecta*. San Diego, CA: Academic Press; 2014 pp 181-186.
132. Sangsin A, Kuptanon C, Srichomthong C, Pongpanich M, Suphapeetiporn K, Shotelersuk V. Two novel compound heterozygous BMP1 mutations in a patient with osteogenesis imperfecta: a case report. *BMC Med Genet.* 2017;18(1):25.
133. Xu XJ, Lv F, Song YW, et al. Novel mutations in BMP1 induce a rare type of osteogenesis imperfecta. *Clin Chim Acta.* 2019;489:21-28.
134. Puig-Hervás MT, Temtamy S, Aglan M, et al. Mutations in PLOD2 cause autosomal-recessive connective tissue disorders within the Bruck syndrome: osteogenesis imperfecta phenotypic spectrum. *Hum Mutat.* 2012;33(10):1444-1449.
135. Morello R, Bertin TK, Chen Y, et al. CRTAP is required for prolyl 3-hydroxylation and mutations cause recessive osteogenesis imperfecta. *Cell.* 2006;127(2):291-304.
136. Barnes AM, Chang W, Morello R, et al. Deficiency of cartilage-associated protein in recessive lethal osteogenesis imperfecta. *N Engl J Med.* 2006;355(26):2757-2764.
137. Fisaletti M, Biggin A, Bennetts B, et al. Novel variant in *Sp7/Osx* associated with recessive osteogenesis imperfecta with bone fragility and hearing impairment. *Bone.* 2018;110:66-75.

138. Lapunzina P, Aglan M, Temtamy S, et al. Identification of a frame-shift mutation in Osterix in a patient with recessive osteogenesis imperfecta. *Am J Hum Genet.* 2010;87(1):110-114.
139. Asharani PV, Keupp K, Semler O, et al. Attenuated BMP1 function compromises osteogenesis, leading to bone fragility in humans and zebrafish. *Am J Hum Genet.* 2012;90(4):661-674.
140. Kague E, Roy P, Asselin G, et al. Osterix/Sp7 limits cranial bone initiation sites and is required for formation of sutures. *Dev Biol.* 2016; 413(2):160-172.
141. Gistelinc C, Witten PE, Huysseune A, et al. Loss of type I collagen telopeptide lysyl hydroxylation causes musculoskeletal abnormalities in a zebrafish model of Bruck syndrome. *J Bone Miner Res.* 2016;31(11):1930-1942.
142. Tonelli F, Cotti S, Leoni L, et al. Crtp and p3h1 knock out zebrafish support defective collagen chaperoning as the cause of their osteogenesis imperfecta phenotype. *Matrix Biol.* 2020;90:40-60.
143. Tomecka MJ, Ethiraj LP, Sanchez LM, Roehl HH, Carney TJ. Clinical pathologies of bone fracture modelled in zebrafish. *Dis Model Mech.* 2019;12(9):dmm037630.
144. Chatani M, Takano Y, Kudo A. Osteoclasts in bone modeling, as revealed by in vivo imaging, are essential for organogenesis in fish. *Dev Biol.* 2011;360(1):96-109.
145. Parichy DM, Ransom DG, Paw B, Zon LI, Johnson SL. An orthologue of the kit-related gene *fms* is required for development of neural crest-derived xanthophores and a subpopulation of adult melanocytes in the zebrafish, *Danio rerio*. *Development.* 2000;127(14): 3031-3044.
146. Jeradi S, Hammerschmidt M. Retinoic acid-induced premature osteoblast-to-preosteocyte transitioning has multiple effects on calvarial development. *Development.* 2016;143(7):1205-1216.
147. Zhang Y, Ji D, Li L, Yang S, Zhang H, Duan X. CIC-7 regulates the pattern and early development of craniofacial bone and tooth. *Theranostics.* 2019;9(5):1387-1400.
148. Gregson CL, Bergen DJM, Leo P, et al. A rare mutation in SMAD9 associated with high bone mass identifies the SMAD-dependent BMP signaling pathway as a potential anabolic target for osteoporosis. *J Bone Miner Res.* 2020;35(1):92-105.
149. Morris JA, Kemp JP, Youlten SE, et al. An atlas of genetic influences on osteoporosis in humans and mice. *Nat Genet.* 2019;51(2): 258-266.
150. Tachmazidou I, Hatzikotoulas K, Southam L, et al. Identification of new therapeutic targets for osteoarthritis through genome-wide analyses of UK Biobank data. *Nat Genet.* 2019;51(2):230-236.
151. McGowan LM, Kague E, Vorster A, Newham E, Cross S, Hammond CL. Wnt16 elicits a protective effect against fractures and supports bone repair in zebrafish. *JBM R Plus.* 2021;e10461. <https://doi.org/10.1002/jbm4.10461>.
152. Bai H, Liu L, An K, et al. CRISPR/Cas9-mediated precise genome modification by a long ssDNA template in zebrafish. *BMC Genomics.* 2020;21(1):67.
153. Aksoy YA, Nguyen DT, Chow S, et al. Chemical reprogramming enhances homology-directed genome editing in zebrafish embryos. *Commun Biol.* 2019;2:198.
154. Zhang Y, Qin W, Lu X, et al. Programmable base editing of zebrafish genome using a modified CRISPR-Cas9 system. *Nat Commun.* 2017; 8(1):118.
155. Marques IJ, Lupi E, Mercader N. Model systems for regeneration: zebrafish. *Development.* 2019;146(18):dev167692.
156. Stock DW. Zebrafish dentition in comparative context. *J Exp Zool B Mol Dev Evol.* 2007;308(5):523-549.
157. Bruneel B, Matha M, Paesen R, Ameloot M, Weninger WJ, Huysseune A. Imaging the zebrafish dentition: from traditional approaches to emerging technologies. *Zebrafish.* 2015;12(1):1-10.
158. Sire JY, Girondot M, Babiar O. Marking zebrafish, *Danio rerio* (cyprinidae), using scale regeneration. *J Exp Zool.* 2000;286(3):297-304.
159. de Vrieze E, van Kessel MA, Peters HM, Spanings FA, Flik G, Metz JR. Prednisolone induces osteoporosis-like phenotype in regenerating zebrafish scales. *Osteoporos Int.* 2014;25(2):567-578.
160. Paul S, Schindler S, Giovannone D, de Millo Terrazzani A, Mariani FV, Crump JG. Ihha induces hybrid cartilage-bone cells during zebrafish jawbone regeneration. *Development.* 2016;143(12):2066-2076.
161. Lin Z, Fateh A, Salem DM, Intini G. Periosteum: biology and applications in craniofacial bone regeneration. *J Dent Res.* 2014;93(2): 109-116.
162. Ohgo S, Ichinose S, Yokota H, Sato-Maeda M, Shoji W, Wada N. Tissue regeneration during lower jaw restoration in zebrafish shows some features of epimorphic regeneration. *Dev Growth Differ.* 2019;61(7-8):419-430.
163. Wang X, He H, Tang W, Zhang XA, Hua X, Yan J. Two origins of blastemal progenitors define blastemal regeneration of zebrafish lower jaw. *PLoS One.* 2012;7(9):e45380.
164. Bereiter-Hahn J, Zylberberg L. Regeneration of teleost fish scale. *Comp Biochem Physiol.* 1993;105:625-641.
165. Iwasaki M, Kuroda J, Kawakami K, Wada H. Epidermal regulation of bone morphogenesis through the development and regeneration of osteoblasts in the zebrafish scale. *Dev Biol.* 2018;437(2):105-119.
166. Sousa S, Afonso N, Bensimon-Brito A, et al. Differentiated skeletal cells contribute to blastema formation during zebrafish fin regeneration. *Development.* 2011;138(18):3897-3905.
167. Stewart S, Stankunas K. Limited dedifferentiation provides replacement tissue during zebrafish fin regeneration. *Dev Biol.* 2012;365(2): 339-349.
168. Singh SP, Holdway JE, Poss KD. Regeneration of amputated zebrafish fin rays from de novo osteoblasts. *Dev Cell.* 2012;22(4):879-886.
169. Ando K, Shibata E, Hans S, Brand M, Kawakami A. Osteoblast production by reserved progenitor cells in zebrafish bone regeneration and maintenance. *Dev Cell.* 2017;43(5):643-50.e3.
170. Lim J, Lee J, Yun H-S, Shin H-I, Park EK. Comparison of bone regeneration rate in flat and long bone defects: calvarial and tibial bone. *Tissue Eng Regen Med.* 2013;10(6):336-340.
171. Shapiro F. Bone development and its relation to fracture repair. The role of mesenchymal osteoblasts and surface osteoblasts. *Eur Cell Mater.* 2008;15:53-76.
172. Zhao H, Feng J, Ho TV, Grimes W, Urata M, Chai Y. The suture provides a niche for mesenchymal stem cells of craniofacial bones. *Nat Cell Biol.* 2015;17(4):386-396.
173. Sehring IM, Jahn C, Weidinger G. Zebrafish fin and heart: what's special about regeneration? *Curr Opin Genet Dev.* 2016;40:48-56.
174. Shao J, Qian X, Zhang C, Xu Z. Fin regeneration from tail segment with musculature, endoskeleton, and scales. *J Exp Zool B Mol Dev Evol.* 2009;312(7):762-769.
175. Pápai N, Kagan F, Csikós G, Kosztelnik M, Vellai T, Varga M. No correlation between endo- and exoskeletal regenerative capacities in teleost species. *Fishes.* 2019;4(4):51.
176. Yoshida K, Kawakami K, Abe G, Tamura K. Zebrafish can regenerate endoskeleton in larval pectoral fin but the regenerative ability declines. *Dev Biol.* 2020;463(2):110-123.
177. Azevedo AS, Grotek B, Jacinto A, Weidinger G, Saude L. The regenerative capacity of the zebrafish caudal fin is not affected by repeated amputations. *PLoS One.* 2011;6(7):e22820.
178. Crotwell PL, Mabee PM. Gene expression patterns underlying proximal-distal skeletal segmentation in late-stage zebrafish, *Danio rerio*. *Dev Dyn.* 2007;236(11):3111-3128.
179. Storm EE, Kingsley DM. GDF5 coordinates bone and joint formation during digit development. *Dev Biol.* 1999;209(1):11-27.
180. Schulte CJ, Allen C, England SJ, Juarez-Morales JL, Lewis KE. Evx1 is required for joint formation in zebrafish fin dermoskeleton. *Dev Dyn.* 2011;240(5):1240-1248.
181. Sims K Jr, Eble DM, Iovine MK. Connexin43 regulates joint location in zebrafish fins. *Dev Biol.* 2009;327(2):410-418.
182. Iovine MK, Johnson SL. Genetic analysis of isometric growth control mechanisms in the zebrafish caudal fin. *Genetics.* 2000;155(3):1321-1329.
183. Iovine MK, Higgins EP, Hindes A, Coblitz B, Johnson SL. Mutations in connexin43 (GJA1) perturb bone growth in zebrafish fins. *Dev Biol.* 2005;278(1):208-219.

184. Goldsmith MI, Fisher S, Waterman R, Johnson SL. Saltatory control of isometric growth in the zebrafish caudal fin is disrupted in long fin and rapunzel mutants. *Dev Biol.* 2003;259(2):303-317.
185. Perathoner S, Daane JM, Henrion U, et al. Bioelectric signaling regulates size in zebrafish fins. *PLoS Genet.* 2014;10(1):e1004080.
186. Harris MP, Daane JM, Lanni J. Through veiled mirrors: fish fins giving insight into size regulation. *Wiley Interdiscip Rev Dev Biol.* 2020: e381.
187. Shibata E, Ando K, Murase E, Kawakami A. Heterogeneous fates and dynamic rearrangement of regenerative epidermis-derived cells during zebrafish fin regeneration. *Development.* 2018;145(8): dev162016.
188. Poleo G, Brown CW, Laforest L, Akimenko MA. Cell proliferation and movement during early fin regeneration in zebrafish. *Dev Dyn.* 2001;221(4):380-390.
189. Akimenko MA, Johnson SL, Westerfield M, Ekker M. Differential induction of four *msx* homeobox genes during fin development and regeneration in zebrafish. *Development.* 1995;121(2):347-357.
190. Wehner D, Cizelsky W, Vasudevarao MD, et al. Wnt/beta-catenin signaling defines organizing centers that orchestrate growth and differentiation of the regenerating zebrafish caudal fin. *Cell Rep.* 2014;6(3):467-481.
191. Nechiporuk A, Keating MT. A proliferation gradient between proximal and *msxb*-expressing distal blastema directs zebrafish fin regeneration. *Development.* 2002;129(11):2607-2617.
192. Poss KD, Keating MT, Nechiporuk A. Tales of regeneration in zebrafish. *Dev Dyn.* 2003;226(2):202-210.
193. Uemoto T, Abe G, Tamura K. Regrowth of zebrafish caudal fin regeneration is determined by the amputated length. *Sci Rep.* 2020;10(1):649.
194. Blum N, Begemann G. Osteoblast de- and redifferentiation are controlled by a dynamic response to retinoic acid during zebrafish fin regeneration. *Development.* 2015;142(17):2894-2903.
195. Mishra R, Sehring I, Cederlund M, Mulaw M, Weidinger G. NF- κ B signaling negatively regulates osteoblast dedifferentiation during zebrafish bone regeneration. *Dev Cell.* 2020;52(2):167-182.e7.
196. Brown AM, Fisher S, Iovine MK. Osteoblast maturation occurs in overlapping proximal-distal compartments during fin regeneration in zebrafish. *Dev Dyn.* 2009;238(11):2922-2928.
197. Tu S, Johnson SL. Fate restriction in the growing and regenerating zebrafish fin. *Dev Cell.* 2011;20(5):725-732.
198. Dasyani M, Tan WH, Sundaram S, et al. Lineage tracing of *col10a1* cells identifies distinct progenitor populations for osteoblasts and joint cells in the regenerating fin of medaka (*Oryzias latipes*). *Dev Biol.* 2019;455(1):85-99.
199. Chassot B, Pury D, Jazwinska A. Zebrafish fin regeneration after cryoinjury-induced tissue damage. *Biol Open.* 2016;5(6):819-828.
200. Geurtzen K, Knopf F. Adult zebrafish injury models to study the effects of prednisolone in regenerating bone tissue. *J Vis Exp.* 2018;140:58429.
201. Park D, Spencer JA, Koh BI, et al. Endogenous bone marrow MSCs are dynamic, fate-restricted participants in bone maintenance and regeneration. *Cell Stem Cell.* 2012;10(3):259-272.
202. Maes C, Kobayashi T, Selig MK, et al. Osteoblast precursors, but not mature osteoblasts, move into developing and fractured bones along with invading blood vessels. *Dev Cell.* 2010;19(2):329-344.
203. Torreggiani E, Matthews BG, Pejda S, et al. Preosteocytes/osteocytes have the potential to dedifferentiate becoming a source of osteoblasts. *PLoS One.* 2013;8(9):e75204.
204. Giovannone D, Paul S, Schindler S, et al. Programmed conversion of hypertrophic chondrocytes into osteoblasts and marrow adipocytes within zebrafish bones. *Elife.* 2019;8:e42736.
205. Jing Y, Zhou X, Han X, et al. Chondrocytes directly transform into bone cells in mandibular condyle growth. *J Dent Res.* 2015;94(12): 1668-1675.
206. Yang L, Tsang KY, Tang HC, Chan D, Cheah KS. Hypertrophic chondrocytes can become osteoblasts and osteocytes in endochondral bone formation. *Proc Natl Acad Sci U S A.* 2014;111(33):12097-12102.
207. Zhou X, von der Mark K, Henry S, Norton W, Adams H, de Crombrughe B. Chondrocytes transdifferentiate into osteoblasts in endochondral bone during development, postnatal growth and fracture healing in mice. *PLoS Genet.* 2014;10(12):e1004820.
208. Nacu E, Tanaka EM. Limb regeneration: a new development? *Annu Rev Cell Dev Biol.* 2011;27:409-440.
209. Zhang H, Wang X, Lyu K, et al. Time point-based integrative analyses of deep-transcriptome identify four signal pathways in blastemal regeneration of zebrafish lower jaw. *Stem Cells.* 2015;33(3):806-818.
210. Vieira WA, McCusker CD. Regenerative models for the integration and regeneration of head skeletal tissues. *Int J Mol Sci.* 2018;19(12):3752.
211. de Vrieze E, Sharif F, Metz JR, Flik G, Richardson MK. Matrix metalloproteinases in osteoclasts of ontogenetic and regenerating zebrafish scales. *Bone.* 2011;48(4):704-712.
212. Langeveld M, Hollak CEM. Bone health in patients with inborn errors of metabolism. *Rev Endocr Metab Disord.* 2018;19(1):81-92.
213. Carnovali M, Banfi G, Mariotti M. Zebrafish models of human skeletal disorders: embryo and adult swimming together. *Biomed Res Int.* 2019;2019:1253710.
214. Mariotti M, Carnovali M, Banfi G. *Danio rerio*: the Janus of the bone from embryo to scale. *Clin Cases Miner Bone Metab.* 2015;12(2): 188-194.
215. Luo S, Yang Y, Chen J, et al. Tanshinol stimulates bone formation and attenuates dexamethasone-induced inhibition of osteogenesis in larval zebrafish. *J Orthop Translat.* 2016;4:35-45.
216. Luo S-Y, Chen J-F, Zhong Z-G, et al. Salvianolic acid B stimulates osteogenesis in dexamethasone-treated zebrafish larvae. *Acta Pharmacol Sin.* 2016;37(10):1370-1380.
217. Huang HX, Lin H, Lan F, Wu YF, Yang ZG, Zhang JJ. Application of bone transgenic zebrafish in anti-osteoporosis chemical screening. *Animal Model Exp Med.* 2018;1(1):53-61.
218. Luo Q, Liu S, Xie L, et al. Resveratrol ameliorates glucocorticoid-induced bone damage in a zebrafish model. *Front Pharmacol.* 2019;10:195.
219. Geurtzen K, Vernet A, Freidin A, et al. Immune suppressive and bone inhibitory effects of prednisolone in growing and regenerating zebrafish tissues. *J Bone Miner Res.* 2017;32(12):2476-2488.
220. Barrett R, Chappell C, Quick M, Fleming A. A rapid, high content, in vivo model of glucocorticoid-induced osteoporosis. *Biotechnol J.* 2006;1(6):651-655.
221. Huo L, Wang L, Yang Z, Li P, Geng D, Xu Y. Prednisolone induces osteoporosis-like phenotypes via focal adhesion signaling pathway in zebrafish larvae. *Biol Open.* 2018;7(7):bio029405.
222. He H, Wang C, Tang Q, Yang F, Xu Y. Possible mechanisms of prednisolone-induced osteoporosis in zebrafish larva. *Biomed Pharmacother.* 2018;101:981-987.
223. Mathew LK, Sengupta S, Kawakami A, et al. Unraveling tissue regeneration pathways using chemical genetics. *J Biol Chem.* 2007;282(48):35202-35210.
224. Chatzopoulou A, Heijmans JP, Burgerhout E, et al. Glucocorticoid-induced attenuation of the inflammatory response in zebrafish. *Endocrinology.* 2016;157(7):2772-2784.
225. Garland MA, Sengupta S, Mathew LK, et al. Glucocorticoid receptor-dependent induction of *cripto-1* (one-eyed pinhead) inhibits zebrafish caudal fin regeneration. *Toxicol Rep.* 2019;6:529-537.
226. Saito Y, Nakamura S, Chinen N, Shimazawa M, Hara H. Effects of anti-osteoporosis drugs against dexamethasone-induced osteoporosis-like phenotype using a zebrafish scale-regeneration model. *J Pharmacol Sci.* 2020;143(2):117-121.
227. Pasqualetti S, Congiu T, Banfi G, Mariotti M. Alendronate rescued osteoporotic phenotype in a model of glucocorticoid-induced osteoporosis in adult zebrafish scale. *Int J Exp Pathol.* 2015;96(1):11-20.
228. Grassi Milano E, Basari F, Chimenti C. Adrenocortical and adrenomedullary homologs in eight species of adult and developing teleosts: morphology, histology, and immunohistochemistry. *Gen Comp Endocrinol.* 1997;108(3):483-496.
229. Keegan CE, Hammer GD. Recent insights into organogenesis of the adrenal cortex. *Trends Endocrinol Metab.* 2002;13(5):200-208.

230. Hollenberg SM, Weinberger C, Ong ES, et al. Primary structure and expression of a functional human glucocorticoid receptor cDNA. *Nature*. 1985;318(6047):635-641.
231. Schaaf MJ, Champagne D, van Laanen IH, et al. Discovery of a functional glucocorticoid receptor beta-isoform in zebrafish. *Endocrinology*. 2008;149(4):1591-1599.
232. Schaaf MJ, Chatzopoulou A, Spink HP. The zebrafish as a model system for glucocorticoid receptor research. *Comp Biochem Physiol A Mol Integr Physiol*. 2009;153(1):75-82.
233. Chatzopoulou A, Schoonheim PJ, Torraca V, Meijer AH, Spink HP, Schaaf MJ. Functional analysis reveals no transcriptional role for the glucocorticoid receptor beta-isoform in zebrafish. *Mol Cell Endocrinol*. 2017;447:61-70.
234. Bamberger CM, Bamberger AM, de Castro M, Chrousos GP. Glucocorticoid receptor beta, a potential endogenous inhibitor of glucocorticoid action in humans. *J Clin Invest*. 1995;95(6):2435-2441.
235. Baker ME. Evolutionary analysis of 11beta-hydroxysteroid dehydrogenase-type 1, -type 2, -type 3 and 17beta-hydroxysteroid dehydrogenase-type 2 in fish. *FEBS Lett*. 2004;574(1-3):167-170.
236. Tsachaki M, Meyer A, Weger B, et al. Absence of 11-keto reduction of cortisone and 11-ketotestosterone in the model organism zebrafish. *J Endocrinol*. 2017;232(2):323-335.
237. Nesan D, Vijayan MM. Role of glucocorticoid in developmental programming: evidence from zebrafish. *Gen Comp Endocrinol*. 2013;181:35-44.
238. Mommsen TP, Vijayan MM, Moon TW. Cortisol in teleosts: dynamics, mechanisms of action, and metabolic regulation. *Rev Fish Biol Fish*. 1999;9(3):211-268.
239. Spackman DH, Riley V. Corticosterone concentrations in the mouse. *Science*. 1978;200(4337):87.
240. Krug RG 2nd, Poshusta TL, Skuster KJ, Berg MR, Gardner SL, Clark KJ. A transgenic zebrafish model for monitoring glucocorticoid receptor activity. *Genes Brain Behav*. 2014;13(5):478-487.
241. Benato F, Colletti E, Skobo T, et al. A living biosensor model to dynamically trace glucocorticoid transcriptional activity during development and adult life in zebrafish. *Mol Cell Endocrinol*. 2014;392(1-2):60-72.
242. Weger BD, Weger M, Nusser M, Brenner-Weiss G, Dickmeis T. A chemical screening system for glucocorticoid stress hormone signaling in an intact vertebrate. *ACS Chem Biol*. 2012;7(7):1178-1183.
243. Schoonheim PJ, Chatzopoulou A, Schaaf MJ. The zebrafish as an in vivo model system for glucocorticoid resistance. *Steroids*. 2010;75(12):918-925.
244. Griffiths BB, Schoonheim PJ, Ziv L, Voelker L, Baier H, Gahtan E. A zebrafish model of glucocorticoid resistance shows serotonergic modulation of the stress response. *Front Behav Neurosci*. 2012;6:68.
245. Facchinello N, Skobo T, Meneghetti G, et al. nr3c1 null mutant zebrafish are viable and reveal DNA-binding-independent activities of the glucocorticoid receptor. *Sci Rep*. 2017;7(1):4371.
246. Faught E, Vijayan MM. The mineralocorticoid receptor is essential for stress axis regulation in zebrafish larvae. *Sci Rep*. 2018;8(1):18081.
247. Faught E, Vijayan MM. Loss of the glucocorticoid receptor in zebrafish improves muscle glucose availability and increases growth. *Am J Physiol Endocrinol Metab*. 2019;316(6):E1093-E1104.
248. Bury NR, Sturm A. Evolution of the corticosteroid receptor signalling pathway in fish. *Gen Comp Endocrinol*. 2007;153(1-3):47-56.
249. Faught E, Vijayan MM. Glucocorticoid and mineralocorticoid receptor activation modulates postnatal growth. *J Endocrinol*. 2020;244(2):261-271.
250. He M, Halima M, Xie Y, Schaaf MJM, Meijer AH, Wang M. Ginsenoside Rg1 acts as a selective glucocorticoid receptor agonist with anti-inflammatory action without affecting tissue regeneration in zebrafish larvae. *Cells*. 2020;9(5):1107.
251. Schmidt JR, Geurtzen K, von Bergen M, Schubert K, Knopf F. Glucocorticoid treatment leads to aberrant ion and macromolecular transport in regenerating zebrafish fins. *Front Endocrinol*. 2019;10:674.
252. Azetsu Y, Chatani M, Dodo Y, et al. Treatment with synthetic glucocorticoid impairs bone metabolism, as revealed by in vivo imaging of osteoblasts and osteoclasts in medaka fish. *Biomed Pharmacother*. 2019;118:109101.
253. Pham CV, Pham TT, Lai TT, et al. Icarin reduces bone loss in a Rankl-induced transgenic medaka (*Oryzias latipes*) model for osteoporosis. *J Fish Biol*. 2020;1-10. <https://doi.org/10.1111/jfb.14241>
254. de Vrieze E, Zethof J, Schulte-Merker S, Flik G, Metz JR. Identification of novel osteogenic compounds by an ex-vivo sp7:Luciferase zebrafish scale assay. *Bone*. 2015;74:106-113.
255. Kobayashi-Sun J, Yamamori S, Kondo M, et al. Uptake of osteoblast-derived extracellular vesicles promotes the differentiation of osteoclasts in the zebrafish scale. *Commun Biol*. 2020;3(1):190.
256. Hygum K, Starup-Linde J, Langdahl BL. Diabetes and bone. *Osteoporos Sarcopenia*. 2019;5(2):29-37.
257. Olsen AS, Sarra MP Jr, Intine RV. Limb regeneration is impaired in an adult zebrafish model of diabetes mellitus. *Wound Repair Regen*. 2010;18(5):532-542.
258. Carnovali M, Luzzi L, Banfi G, Mariotti M. Chronic hyperglycemia affects bone metabolism in adult zebrafish scale model. *Endocrine*. 2016;54(3):808-817.
259. Carnovali M, Luzzi L, Terruzzi I, Banfi G, Mariotti M. Liquiritigenin reduces blood glucose level and bone adverse effects in hyperglycemic adult zebrafish. *Nutrients*. 2019;11(5):1042.
260. Lock EJ, Waagbø R, Wendelaar Bonga S, Flik G. The significance of vitamin D for fish: a review. *Aquacult Nutr*. 2010;16(1):100-116.
261. Nachtrab G, Kikuchi K, Tornini VA, Poss KD. Transcriptional components of anteroposterior positional information during zebrafish fin regeneration. *Development*. 2013;140(18):3754-3764.
262. Chen A, Han Y, Poss KD. Regulation of zebrafish fin regeneration by vitamin D signaling. *Dev Dyn*. 2020;1-10. <https://doi.org/10.1002/dvdy.261>.
263. Fleming A, Sato M, Goldsmith P. High-throughput in vivo screening for bone anabolic compounds with zebrafish. *J Biomol Screen*. 2005;10(8):823-831.
264. Tarasco M, Laize V, Carreira J, Cancela ML, Gavaia PJ. The zebrafish operculum: a powerful system to assess osteogenic bioactivities of molecules with pharmacological and toxicological relevance. *Comp Biochem Physiol C Toxicol Pharmacol*. 2017;197:45-52.
265. Carvalho FR, Fernandes AR, Cancela ML, Gavaia PJ. Improved regeneration and de novo bone formation in a diabetic zebrafish model treated with paricalcitol and cinacalcet. *Wound Repair Regen*. 2017;25(3):432-442.
266. Yin JJ, Selander K, Chirgwin JM, et al. TGF-beta signaling blockade inhibits PTHrP secretion by breast cancer cells and bone metastases development. *J Clin Invest*. 1999;103(2):197-206.
267. Hiraga T, Myoui A, Hashimoto N, et al. Bone-derived IGF mediates crosstalk between bone and breast cancer cells in bony metastases. *Cancer Res*. 2012;72(16):4238-4249.
268. Schneider JG, Amend SR, Weillbaecher KN. Integrins and bone metastasis: integrating tumor cell and stromal cell interactions. *Bone*. 2011;48(1):54-65.
269. Pazolli E, Luo X, Brehm S, et al. Senescent stromal-derived osteopontin promotes preneoplastic cell growth. *Cancer Res*. 2009;69(3):1230-1239.
270. Kaplan RN, Riba RD, Zacharoulis S, et al. VEGFR1-positive haematopoietic bone marrow progenitors initiate the pre-metastatic niche. *Nature*. 2005;438(7069):820-827.
271. Guise T. Examining the metastatic niche: targeting the microenvironment. *Semin Oncol*. 2010;37(Suppl 2):S2-S14.
272. Karlsson T, Sundar R, Widmark A, Landstrom M, Persson E. Osteoblast-derived factors promote metastatic potential in human prostate cancer cells, in part via non-canonical transforming growth factor beta (TGFbeta) signaling. *Prostate*. 2018;78(6):446-456.
273. Bussard KM, Venzon DJ, Mastro AM. Osteoblasts are a major source of inflammatory cytokines in the tumor microenvironment of bone metastatic breast cancer. *J Cell Biochem*. 2010;111(5):1138-1148.
274. Schmid-Alliana A, Schmid-Antomarchi H, Al-Sahlanee R, Lagadec P, Scimeca JC, Verron E. Understanding the progression of bone

- metastases to identify novel therapeutic targets. *Int J Mol Sci*. 2018; 19(1):148.
275. He S, Lamers GE, Beenakker JW, et al. Neutrophil-mediated experimental metastasis is enhanced by VEGFR inhibition in a zebrafish xenograft model. *J Pathol*. 2012;227(4):431-445.
 276. Sacco A, Roccaro AM, Ma D, et al. Cancer cell dissemination and homing to the bone marrow in a zebrafish model. *Cancer Res*. 2016;76(2):463-471.
 277. Paul CD, Bishop K, Devine A, et al. Tissue architectural cues drive organ targeting of tumor cells in zebrafish. *Cell Syst*. 2019;9(2): 187-206.e16.
 278. Blaser BW, Moore JL, Hagedorn EJ, et al. CXCR1 remodels the vascular niche to promote hematopoietic stem and progenitor cell engraftment. *J Exp Med*. 2017;214(4):1011-1027.
 279. Sun YX, Schneider A, Jung Y, et al. Skeletal localization and neutralization of the SDF-1(CXCL12)/CXCR4 axis blocks prostate cancer metastasis and growth in osseous sites in vivo. *J Bone Miner Res*. 2005;20(2):318-329.
 280. Chinni SR, Sivalogan S, Dong Z, et al. CXCL12/CXCR4 signaling activates Akt-1 and MMP-9 expression in prostate cancer cells: the role of bone microenvironment-associated CXCL12. *Prostate*. 2006;66(1):32-48.
 281. Wang J, Loberg R, Taichman RS. The pivotal role of CXCL12 (SDF-1)/CXCR4 axis in bone metastasis. *Cancer Metastasis Rev*. 2006;25(4):573-587.
 282. Tulotta C, Snaar-Jagalska BE. CXCR4 signalling, metastasis and immunotherapy: zebrafish xenograft model as translational tool for anti-cancer discovery. *J Cancer Metastasis Treat*. 2019;5:74.
 283. Tulotta C, Stefanescu C, Beletkaia E, et al. Inhibition of signaling between human CXCR4 and zebrafish ligands by the small molecule IT1t impairs the formation of triple-negative breast cancer early metastases in a zebrafish xenograft model. *Dis Model Mech*. 2016;9(2):141-153.
 284. Tulotta C, Stefanescu C, Chen Q, Torracca V, Meijer AH, Snaar-Jagalska BE. CXCR4 signaling regulates metastatic onset by controlling neutrophil motility and response to malignant cells. *Sci Rep*. 2019;9(1):2399.
 285. Butko E, Distel M, Pouget C, et al. Gata2b is a restricted early regulator of hemogenic endothelium in the zebrafish embryo. *Development*. 2015;142(6):1050-1061.
 286. Tsai FY, Orkin SH. Transcription factor GATA-2 is required for proliferation/survival of early hematopoietic cells and mast cell formation, but not for erythroid and myeloid terminal differentiation. *Blood*. 1997;89(10):3636-3643.
 287. Rodriguez-Bravo V, Carceles-Cordon M, Hoshida Y, Cordon-Cardo C, Galsky MD, Domingo-Domenech J. The role of GATA2 in lethal prostate cancer aggressiveness. *Nat Rev Urol*. 2017;14(1):38-48.
 288. Tamplin OJ, Durand EM, Carr LA, et al. Hematopoietic stem cell arrival triggers dynamic remodeling of the perivascular niche. *Cell*. 2015;160(1-2):241-252.
 289. Mahony CB, Fish RJ, Pasche C, Bertrand JY. tfec controls the hematopoietic stem cell vascular niche during zebrafish embryogenesis. *Blood*. 2016;128(10):1336-1345.
 290. Mahony CB, Pasche C, Bertrand JY. Oncostatin M and kit-ligand control hematopoietic stem cell fate during zebrafish embryogenesis. *Stem Cell Reports*. 2018;10(6):1920-1934.
 291. Xue Y, Lv J, Zhang C, Wang L, Ma D, Liu F. The vascular niche regulates hematopoietic stem and progenitor cell lodgment and expansion via klf6a-ccl25b. *Dev Cell*. 2017;42(4):349-362.e4.
 292. Jin C, Shang Y, Yan H, Hao J. High levels of TFEC expression associated with aggressive clinical features in ovarian cancer. *Int J Clin Exp Med*. 2018;11(10):10692-10702.
 293. Rehli M, Sulzbacher S, Pape S, et al. Transcription factor Tfec contributes to the IL-4-inducible expression of a small group of genes in mouse macrophages including the granulocyte colony-stimulating factor receptor. *J Immunol*. 2005;174(11):7111-7122.
 294. West NR, Owens BMJ, Hegazy AN. The oncostatin M-stromal cell axis in health and disease. *Scand J Immunol*. 2018;88(3):e12694.
 295. Bolin C, Tawara K, Sutherland C, et al. Oncostatin m promotes mammary tumor metastasis to bone and osteolytic bone degradation. *Genes Cancer*. 2012;3(2):117-130.
 296. Borsig L, Wolf MJ, Roblek M, Lorentzen A, Heikenwalder M. Inflammatory chemokines and metastasis: tracing the accessory. *Oncogene*. 2014;33(25):3217-3224.
 297. Scheibenbogen C, Mohler T, Haefele J, Hunstein W, Keilholz U. Serum interleukin-8 (IL-8) is elevated in patients with metastatic melanoma and correlates with tumour load. *Melanoma Res*. 1995;5(3):179-181.
 298. Costanzo-Garvey DL, Keeley T, Case AJ, et al. Neutrophils are mediators of metastatic prostate cancer progression in bone. *Cancer Immunol Immunother*. 2020;69(6):1113-1130.
 299. Lo CH, Lynch CC. Multifaceted roles for macrophages in prostate Cancer skeletal metastasis. *Front Endocrinol (Lausanne)*. 2018;9:247.
 300. Beckwith LG, Moore JL, Tsao-Wu GS, Harshbarger JC, Cheng KC. Ethylnitrosourea induces neoplasia in zebrafish (*Danio rerio*). *Lab Invest*. 2000;80(3):379-385.
 301. Berghmans S, Murphey RD, Wienholds E, et al. tp53 mutant zebrafish develop malignant peripheral nerve sheath tumors. *Proc Natl Acad Sci U S A*. 2005;102(2):407-412.
 302. Patton EE, Widlund HR, Kutok JL, et al. BRAF mutations are sufficient to promote nevi formation and cooperate with p53 in the genesis of melanoma. *Curr Biol*. 2005;15(3):249-254.
 303. Osmani N, Goetz JG. Multiscale imaging of metastasis in zebrafish. *Trends Cancer*. 2019;5(12):766-778.
 304. van der Ent W, Burrello C, de Lange MJ, et al. Embryonic zebrafish: different phenotypes after injection of human Uveal melanoma cells. *Ocul Oncol Pathol*. 2015;1(3):170-181.
 305. Marques IJ, Weiss FU, Vlecken DH, et al. Metastatic behaviour of primary human tumours in a zebrafish xenotransplantation model. *BMC Cancer*. 2009;9:128.
 306. Kirchberger S, Sturtzel C, Pascoal S, Distel M. Quo natus, Danio?—Recent Progress in modeling cancer in zebrafish. *Front Oncol*. 2017;7:186.
 307. Liu C, Zhang Y, Lim S, et al. A zebrafish model discovers a novel mechanism of stromal fibroblast-mediated cancer metastasis. *Clin Cancer Res*. 2017;23(16):4769-4779.
 308. Chen L, Boleslaw Olszewski M, Kruihof-de Julio M, Snaar-Jagalska BE. Zebrafish microenvironment elevates EMT and CSC-like phenotype of engrafted prostate Cancer cells. *Cells*. 2020;9(4):797.
 309. Chen L, De Menna M, Groenewoud A, Thalmann GN, Kruihof-de Julio M, Snaar-Jagalska BE. A NF-kB-Activin a signaling axis enhances prostate cancer metastasis. *Oncogene*. 2020;39(8):1634-1651.
 310. de Boeck M, Cui C, Mulder AA, Jost CR, Ikeno S, Ten Dijke P. Smad6 determines BMP-regulated invasive behaviour of breast cancer cells in a zebrafish xenograft model. *Sci Rep*. 2016;6:24968.
 311. Li Y, Drabsch Y, Pujuguet P, et al. Genetic depletion and pharmacological targeting of alphav integrin in breast cancer cells impairs metastasis in zebrafish and mouse xenograft models. *Breast Cancer Res*. 2015;17:28.
 312. Roccaro AM, Sacco A, Purschke WG, et al. SDF-1 inhibition targets the bone marrow niche for cancer therapy. *Cell Rep*. 2014;9(1):118-128.
 313. Zhang XG, Klein B, Bataille R. Interleukin-6 is a potent myeloma-cell growth factor in patients with aggressive multiple myeloma. *Blood*. 1989;74(1):11-13.
 314. Vidriales MB, Anderson KC. Adhesion of multiple myeloma cells to the bone marrow microenvironment: implications for future therapeutic strategies. *Mol Med Today*. 1996;2(10):425-431.
 315. Giuliani N, Storti P, Bolzoni M, Palma BD, Bonomini S. Angiogenesis and multiple myeloma. *Cancer Microenviron*. 2011;4(3):325-337.
 316. Pandey MK, Rastogi S, Kale VP, Gowda T, Amin SG. Targeting CXCL12/CXCR4 axis in multiple myeloma. *J Hematol Thrombo*. 2014;2(5):1-10.
 317. Soodgupta D, Zhou H, Beaino W, et al. Ex vivo and in vivo evaluation of overexpressed VLA-4 in multiple myeloma using LLP2A imaging agents. *J Nucl Med*. 2016;57(4):640-645.

318. Park SY, Wolfram P, Canty K, et al. Focal adhesion kinase regulates the localization and retention of pro-B cells in bone marrow micro-environments. *J Immunol.* 2013;190(3):1094-1102.
319. Pritchard EM, Stewart E, Zhu F, et al. Pharmacokinetics and efficacy of the spleen tyrosine kinase inhibitor r406 after ocular delivery for retinoblastoma. *Pharm Res.* 2014;31(11):3060-3072.
320. Ghotra VP, He S, van der Horst G, et al. SYK is a candidate kinase target for the treatment of advanced prostate cancer. *Cancer Res.* 2015;75(1):230-240.
321. Ikonomopoulou MP, Fernandez-Rojo MA, Pineda SS, et al. Gomesin inhibits melanoma growth by manipulating key signaling cascades that control cell death and proliferation. *Sci Rep.* 2018;8(1):11519.